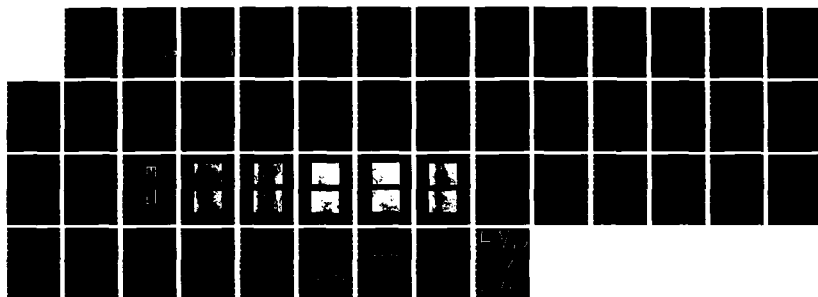
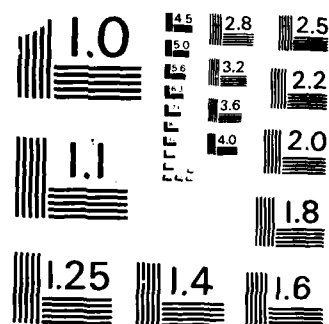


AD-A175 123

AN INTERDISCIPLINARY APPROACH TO PREDICTIVE MODELING OF 1/1  
STRUCTURAL ADHESION (U) VIRGINIA TECH CENTER FOR  
ADHESION SCIENCE BLACKSBURG J A FILBEY ET AL. OCT 86  
CAS/CHEM-86-13 N00014-82-K-0185 F/G 11/1 NL

UNCLASSIFIED





MICROCOPY RESOLUTION TEST CHART  
NATIONAL BUREAU OF STANDARDS-1963-A

AD-A175 123

12

# VIRGINIA TECH CENTER FOR ADHESION SCIENCE

CAS/CHEM-86-13  
CAS/CHEM-12-86, No. 95

October 1986

## ANNUAL REPORT

AN INTERDISCIPLINARY APPROACH TO PREDICTIVE MODELING  
OF STRUCTURAL ADHESIVE BONDING

CHARACTERIZATION OF Ti-6Al-4V OXIDES AND THE  
ADHESIVE/OXIDE INTERPHASE

by

J. A. Filbey  
and  
J. P. Wightman

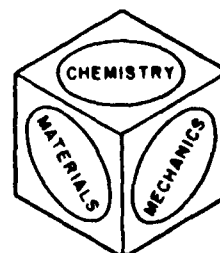
Prepared under Contract No. N00014-82-K-0185 P00002  
Dr. Larry H. Peebles, Jr., Project Monitor  
Office of Naval Research  
Code 431  
800 N. Quincy Street  
Arlington, VA 22217



VIRGINIA POLYTECHNIC INSTITUTE  
AND STATE UNIVERSITY

216 NORRIS HALL  
BLACKSBURG, VIRGINIA 24061

Telephone: (703) 961-6824  
TLX: EZLINK 9103331861  
VPI-BKS



DTIC FILE COPY

This document has been approved  
for publication and sale; its  
distribution is unlimited.

86 12 15 044

12

---

# VIRGINIA TECH CENTER FOR ADHESION SCIENCE

---

CAS/CHEM-86-13  
CAS/CHEM-12-86, No. 95

October 1986

## ANNUAL REPORT

AN INTERDISCIPLINARY APPROACH TO PREDICTIVE MODELING  
OF STRUCTURAL ADHESIVE BONDING

CHARACTERIZATION OF Ti-6Al-4V OXIDES AND THE  
ADHESIVE/OXIDE INTERPHASE

by

J. A. Filbey  
and  
J. P. Wightman

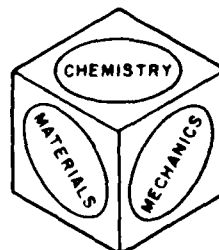
Prepared under Contract No. N00014-82-K-0185 P00002  
Dr. Larry H. Peebles, Jr., Project Monitor  
Office of Naval Research  
Code 431  
800 N. Quincy Street  
Arlington, VA 22217

OTIC  
DEC 1 1986  
E

VIRGINIA POLYTECHNIC INSTITUTE  
AND STATE UNIVERSITY

216 NORRIS HALL  
BLACKSBURG, VIRGINIA 24061

Telephone: (703) 961-6824  
TLX: EZLINK 9103331861  
VPI-BKS



---

OTIC FILE COPY

Approved  
Date

86 10 10

## REPORT DOCUMENTATION PAGE

1a. REPORT SECURITY CLASSIFICATION Unclassified			1b. RESTRICTIVE MARKINGS																								
2a. SECURITY CLASSIFICATION AUTHORITY			3. DISTRIBUTION/AVAILABILITY OF REPORT Distribution Unlimited																								
2b. DECLASSIFICATION/DOWNGRADING SCHEDULE																											
4. PERFORMING ORGANIZATION REPORT NUMBER(S) CAS/CHEM-86-13 CAS/CHEM-12-86, No. 95			5. MONITORING ORGANIZATION REPORT NUMBER(S)																								
6a. NAME OF PERFORMING ORGANIZATION Virginia Polytechnic Institute and State University		6b. OFFICE SYMBOL (If applicable)		7a. NAME OF MONITORING ORGANIZATION																							
6c. ADDRESS (City, State, and ZIP Code) Center for Adhesion Science and Department of Engineering Science & Mechanics Blacksburg, VA 24061			7b. ADDRESS (City, State, and ZIP Code)																								
8a. NAME OF FUNDING/SPONSORING ORGANIZATION Office of Naval Research		8b. OFFICE SYMBOL (If applicable)		9. PROCUREMENT INSTRUMENT IDENTIFICATION NUMBER N00014-82-K-0185 P00002																							
8c. ADDRESS (City, State, and ZIP Code) 800 N. Quincy St. Arlington, VA 22217			10. SOURCE OF FUNDING NUMBERS																								
			PROGRAM ELEMENT NO	PROJECT NO	TASK NO																						
			WORK UNIT ACCESSION NO.																								
11. TITLE (Include Security Classification) An Interdisciplinary Approach to Predictive Modeling of Structural Adhesive Bonding Characterization of Ti-6Al-4V Oxides and the Adhesive/Oxide Interphase (Unclassified)																											
12. PERSONAL AUTHOR(S) Filbey, J. A. and Wightman, J. P.																											
13a. TYPE OF REPORT Annual Report		13b. TIME COVERED FROM 3/86 TO 9/86		14. DATE OF REPORT (Year, Month, Day) 10/86																							
15. PAGE COUNT 44																											
16. SUPPLEMENTARY NOTATION																											
17. COSATI CODES			18. SUBJECT TERMS (Continue on reverse if necessary and identify by block number)																								
FIELD	GROUP	SUB-GROUP																									
19. ABSTRACT (Continue on reverse if necessary and identify by block number)			<table border="1"> <tr> <td colspan="2">Accession For</td> </tr> <tr> <td>NTIS GRA&amp;I</td> <td><input checked="" type="checkbox"/></td> </tr> <tr> <td>DTIC TAB</td> <td><input type="checkbox"/></td> </tr> <tr> <td>Unannounced</td> <td><input type="checkbox"/></td> </tr> <tr> <td>Justification</td> <td></td> </tr> <tr> <td colspan="2">By _____</td> </tr> <tr> <td colspan="2">Distribution / _____</td> </tr> <tr> <td colspan="2">Availability Codes</td> </tr> <tr> <td colspan="2">_____</td> </tr> <tr> <td colspan="2">Dist _____</td> </tr> <tr> <td colspan="2">A-1</td> </tr> </table>			Accession For		NTIS GRA&I	<input checked="" type="checkbox"/>	DTIC TAB	<input type="checkbox"/>	Unannounced	<input type="checkbox"/>	Justification		By _____		Distribution / _____		Availability Codes		_____		Dist _____		A-1	
Accession For																											
NTIS GRA&I	<input checked="" type="checkbox"/>																										
DTIC TAB	<input type="checkbox"/>																										
Unannounced	<input type="checkbox"/>																										
Justification																											
By _____																											
Distribution / _____																											
Availability Codes																											
_____																											
Dist _____																											
A-1																											
20. DISTRIBUTION/AVAILABILITY OF ABSTRACT <input checked="" type="checkbox"/> UNCLASSIFIED/UNLIMITED <input type="checkbox"/> SAME AS RPT <input type="checkbox"/> DTIC USERS			21. ABSTRACT SECURITY CLASSIFICATION																								
22a. NAME OF RESPONSIBLE INDIVIDUAL			22b. TELEPHONE (Include Area Code)		22c. OFFICE SYMBOL																						



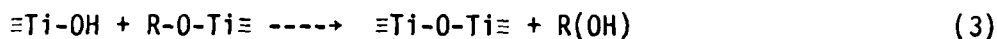
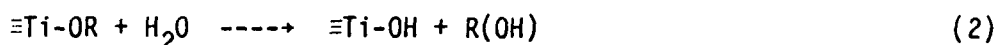
## I. INTRODUCTION

→The hydrothermal durability of adhesive bonds is currently an active area of research. This work focuses on titanium/epoxy bonding using metal alkoxide primers as adhesive promoters. Pike showed that sec-butyl aluminum alkoxide enhances the durability of PAA (phosphoric acid anodized) and FPL (Forest Products Lab) etched 2024 aluminum bonded with the wedge test using epoxy adhesives [1]. No variation in bond performance was observed when the cure temperature of the alkoxide film was varied [1].

Hydrolysis of metal alkoxides occurs readily in the presence of moisture as indicated by the equation,

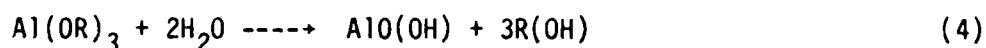


Titanium alkoxide hydrolysis is complex because it involves simultaneous hydrolysis and polymerization as shown below.



These reactions form polycondensates dependent on the water/alkoxide ratio, hydrolysis medium, temperature, and the nature of the alkyl group [2,3]:

Aluminum alkoxides hydrolyze to monohydroxides initially and later convert to trihydroxides [4] as shown below.



> In hot water, a crystalline boehmite is formed, whereas an amorphous hydroxide is formed in cold water. Both hydroxides will convert to aluminum oxide at 500°C [3].

This report encompasses characterization and adhesive bonding studies of three metal alkoxide primers: tetra n-butyl titanate, TNBT; tetra isopropyl titanate, TIPT; and sec-butyl aluminum alkoxide, E-8385. The films have been characterized by XPS (x-ray photoelectron spectroscopy), STEM (scanning transmission electron microscopy), and FTIR (Fourier transform infrared spectroscopy). Adhesive bonding included the wedge test and the stress durability test to determine time to failure and locus of failure. It was concluded that E-8385 promotes the durability of P/F pretreated adherends, whereas the titanates provide no improvement.

## II. EXPERIMENTAL

### A. Surface Pretreatments

Oxide layers were created on the Ti-6-4 surfaces of the wedge and stress durability samples by one of the following pretreatments: a 10 volt chromic acid anodization (CAA), a 10 volt sodium hydroxide anodization (SHA), a phosphate-fluoride acidic etch (P/F), or the TURCO 5578 basic etch. The procedures for each of these pretreatments are listed in Appendix A.

### B. Alkoxide Primer Preparation

Three alkoxide primers were used in this study - E-8385, a sec-butyl aluminum alkoxide; TNBT, a tetra n-butyl titanate; and TIPT, a tetra isopropyl titanate all obtained from Stauffer Chemical Company. One weight percent solutions in dry or water saturated toluene were made in a glove bag purged with dry nitrogen. The toluene was dried by stirring over calcium

hydride overnight and distilling into a flask containing activated molecular sieves. Toluene was saturated with water by shaking a separatory funnel with approximately equal volumes of toluene and water and allowing the mixture to equilibrate overnight.

Five coats of the alkoxide solutions were brushed on the following substrates - ferrotype plates for XPS and FTIR analyses, Ti-6-4 foil for STEM observation and Ti-6-4 wedge or lap shear coupons for durability testing. A 1 wt % solution of E-8385 in wet toluene was also spun coat onto ferrotype plates for XPS analysis.

#### C. XPS

XPS analysis was obtained on a PHI 5300 system, using a Mg anode. Samples were scanned from 0 to 1000 ev. Narrow scans were routinely made on any significant peaks seen in the wide scan spectra.

In addition to the 90° take-off angle, the alkoxide films were also narrow scanned at 30° and 10°. This provides a shallower sampling depth, as illustrated in Figure 1.

#### D. STEM

STEM pictures were obtained on a Phillips EM-420T electron microscope.

#### E. FTIR

A Nicolet 5DX FTIR spectrophotometer was used with the grazing angle specular reflectance attachment shown in Figure 2. The chamber was purged with nitrogen gas for 30 minutes before a spectrum was obtained.

#### F. Bonding

Wedge samples were pretreated, primed, and bonded with FM-300U epoxy at



175°C (350°F) and 1.72 MPa (250 psi), for 1.5 hours from a room temperature start. Two layers of epoxy were used with three layers of teflon film used as spacers, yielding a bond thickness of 0.0381 cm (0.015 in.). After bonding, a wedge made of Ti-6-4 was driven into one end of the sample, causing an initial crack to propagate. The sample was then placed in an environment, held at 80°C and 95% rh. Periodically, the position of the crack was measured with a ruler.

Lap shear joints were bonded with four layers of FM-300U at 175°C (350°F) and 13.8 MPa (2,000 psi) for 1.5 hours from a room temperature start. These lap shear joints were used in a stress-durability tester, shown in Figure 3, where 40% of breaking strength was loaded on each bond and placed in 80°C 95% r.h. (relative humidity).

### III. RESULTS AND DISCUSSION

#### A. Characterization of Alkoxide Films

##### 1. XPS

##### a. TNBT

The effect of cure temperature on surface composition was made for TNBT in dry toluene. Table I lists the elements detected, the binding energies (BE in eV), the atomic percents (AP) and the atomic percent ratios. As indicated by the C/Ti ratios, significantly less carbon was detected on the 300°C cured film than on the 25°C cured film. The decrease in carbon could be due to less contamination or a more complete reaction of the alkoxide to oxide and alcohol with subsequent release of alcohol (see equation (1)). The carbon appeared to be close to the surface as the C/Ti ratio increased with decreasing sampling depth.

No chromium from the ferrotype plate substrate was detected in the 25°C cured film indicating a film thicker than 5 nm. In contrast to the 25°C cured film, chromium was detected on the 300°C cured film, indicating a film less than 5 nm thick or a discontinuous film.

Because chromium was detected on the 300°C film, the film was analyzed at two other take-off angles of 30° and 10° to probe regions closer to the surface. The oxygen 1s photopeak had a shoulder on the high binding energy side which increased as the take-off angle decreased. This oxygen shoulder was primarily due to an O-Si bond. The Si/Ti ratio increased with decreasing take-off angle indicating the silicon was a surface contaminant.

b. TIPT

The cure temperature also affected the surface composition of the TIPT film. Table II lists the elements detected, the binding energies, the atomic percents and the atomic percent ratios. Less carbon was detected on the 300°C cured film than on the 25°C cured film. The silicon contamination was also present on these films and the Si/Ti ratio increased as the take-off angle decreased. The oxygen 1s photopeak had a high binding energy shoulder which increased as the take-off angle decreased. Similar to the TNBT film, the 25°C cured TIPT film showed no chromium, where the 300°C cured film did. The Cr/Ti ratio decreased with decreasing take-off angle.

c. E-8385

The effect of cure temperature, solvent moisture and film application method was studied with E-8385 films. Table III lists the elements detected, the binding energies, the atomic percents and the atomic percent ratios. In contrast to the titanate films, chromium was detected on both the 25°C and

300°C cured films. In all cases, the Cr/Al ratio was two to four times larger in the 25°C cured films than in the 300°C cured films.

The aluminum 2p photopeak in the 25°C cured film from wet toluene was a doublet indicating two bonding states of aluminum. At a 30° take-off angle, the low binding energy component of the aluminum peak had decreased to a shoulder. At the 10° take-off angle, the aluminum peak, still broad, did not distinctly show two components. The change in the aluminum peak with take-off angle could be due to an aluminum hydroxide or hydrated aluminum oxide layer covering an aluminum oxide layer. The O/Al ratio increased as the take-off angle decreased, which was expected if an overlayer of  $\text{Al}(\text{OH})_3$  was covering a sublayer of  $\text{Al}_2\text{O}_3$ . The binding energies of oxygen and aluminum for the 25°C cured film from dry toluene were higher than that expected for  $\text{Al}_2\text{O}_3$ , indicating an aluminum hydroxide. The binding energies of aluminum for the 300°C cured films from both the wet and dry toluene correspond to  $\text{Al}_2\text{O}_3$ .

For both the 25°C and 300°C cured films, the Cr/Al ratio was higher in the wet toluene films than the dry toluene films. The difference in the Cr/Al ratio indicated that the films formed from the wet toluene were thinner than those formed from dry toluene. This difference in thickness can be explained using equation (1). If the water in the toluene reacted with the aluminum alkoxide in solution, before being deposited on the ferrotype plate, less alkoxide was in the solution when it was applied, thus a thinner film resulted.

The origin of the silicon observed in the cured films was unclear. For the 25°C cured films, the Si/Al ratio increased slightly as the take-off angle decreased. This trend was not observed for the 300°C cured films. One possible source of the silicon was from the brushes used to apply the films. Therefore, E-8385 films were spun coat onto ferrotype plates from wet toluene solutions. The Si/Al ratios were five times less than the brush coated films,

while the Cr/Al films were comparable, indicating similar thickness films. Thus, the observed silicon seems to be coming from the brush used to apply the coating.

## 2. STEM

TNBT, TIPT and E-8385 were coated onto as received Ti-6-4 foil and cured at either 25°C or 300°C to compare surface topographies and to look for film discontinuities. In all cases the substrate below the film was not observed. Figures 4 and 5 are photomicrographs of two of the films cured at 25°C. All three films possessed the same topography at 6400 X. However, at 50,000 X, the E-8385 film appeared rougher than the TNBT or TIPT films as shown in Figures 6 and 7. Figures 8 and 9 are photomicrographs of two of the films cured at 300°C. Again, all three films possess the same topography at 6400 X, but at 50,000 X seen in Figures 10 and 11, the E-8385 film surface contains many more features. The 300°C cure films differ from the 25°C cure films. Particle-type features appear on the 300°C cure films which are not observed on the 25°C cure films. Figures 12 and 13 are photomicrographs of E-8385 film from wet toluene, cured at 25° and 500°C. The topography of the films differs dramatically between the two cure temperatures. Water in the toluene caused a different film topography from the dry toluene films. Perhaps a hydroxide, a product of a water-alkoxide reaction, was deposited on the surface of the film.

## 3. Grazing Angle FTIR

Grazing angle FTIR was also used to compare the effects of cure temperature and solvent moisture content on the alkoxide films. Figures 14 to 17 show the FTIR spectra for the TNBT and TIPT films at 25°C and 300°C

cure temperatures. The C-H stretch region (ca.  $2950\text{ cm}^{-1}$ ) was present in the  $25^{\circ}\text{C}$  cured films, but not in the  $300^{\circ}\text{C}$  cure films. The (C-O)Ti region (ca.  $1050\text{ cm}^{-1}$ ) was diminished following  $300^{\circ}\text{C}$  cure. XPS data also showed a reduction in the carbon content following  $300^{\circ}\text{C}$  cure.

Figures 18 and 21 show the FTIR spectra for E-8385 films from dry and wet toluene at  $25^{\circ}\text{C}$  and  $300^{\circ}\text{C}$  cure temperatures. As with the titanate films, the C-H stretch region disappears after cure at  $300^{\circ}\text{C}$  and the intensity of the (C-O)Ti absorbance is diminished.

#### B. Adhesive Bonding

Alkoxide primers are currently being investigated in different laboratories as adhesion promoters. Studies of both characterization and adhesive bonding are necessary. The P/F pretreatment shows poor durability compared to CAA, SHA, and TURCO pretreatments [5]. Because of its poor durability, the P/F pretreatment was chosen as the first surface to apply the alkoxide primers. It was previously shown that P/F wedge samples primed with E-8385 and immersed in  $95^{\circ}\text{C}$  water, were more durable than when no primer was used [6]. However, the ten fold improvement still did not equal the durability of the other pretreatments without primer. Further studies are presented here using an  $80^{\circ}\text{C}$ , 95% r.h. environment, where time to failure and locus of failure were investigated. Three alkoxide primers, TNBT, TIPT, and E-8385, were brush coated onto P/F wedge samples and cured at  $25^{\circ}\text{C}$  and  $300^{\circ}\text{C}$ . The titanate primers created markedly less durable bonds than the aluminum alkoxide primed bonds. The  $25^{\circ}\text{C}$  cured TNBT wedge samples failed upon wedge insertion. The  $300^{\circ}\text{C}$  cured TNBT wedge samples showed crack propagation to failure within 2.5 hours. The TIPT also showed rapid crack propagation with the  $25^{\circ}\text{C}$  cured film samples failing somewhat more rapidly than the  $300^{\circ}\text{C}$  cured film. Figure 22 shows the crack length vs. time for the titanate primers.

In contrast to the titanate primers, the aluminum alkoxide primer, E-8385, showed a significant enhancement of the P/F durability. In 14 days, the crack still had not propagated to failure as shown in Figure 23. The crack usually propagated to failure within 24 hours for the unprimed P/F surfaces [5]. At 80°C, 95% rh, the E-8385 greatly enhances the durability of the P/F surface.

Stress durability tests have also been done on unprimed and alkoxide primed surfaces. Figure 24 shows time to failure windows (in days) for the primed and unprimed surfaces. These stress durability tests agree with the wedge test results in relative times to failure for the P/F and P/F with E-8385 surfaces. When the CAA surface was primed with E-8385, the durability was similar to primed P/F bonds. The unprimed CAA showed better durability than the primed CAA.

Failure surfaces were examined by XPS to determine the locus of failure. Table IV lists the elements detected, the binding energies, and the atomic percents of the unprimed P/F surfaces from the wedge and stress durability tests. Both metal failure surfaces (MFS) contained titanium, oxygen, and no bromine (present in the epoxy) whereas the adhesive failure surfaces (AFS) contained carbon, oxygen and bromine. The binding energies of the oxygen are indicative of titanium oxide on the MFS and of the epoxy on the AFS. Nitrogen, presumably from the epoxy, was present on the MFS indicating that some type of chemical interaction had occurred; however, in general the failure appeared to be interfacial for both the stress durability and the wedge test as shown schematically in Figure 25.

The TURCO pretreatment, tested by the stress durability test also failed interfacially. Table V lists the elements detected, the binding energies, and the atomic percents. As with the P/F surface, the MFS contained no bromine, with titanium and oxygen present with binding energies in agreement with pretreated titanium. The AFS contained carbon, oxygen and bromine.

When alkoxide primers were coated onto P/F pretreated surfaces, the locus of failure was no longer interfacial as with the P/F surface. XPS analysis of the MFS and AFS of TNBT coated wedge samples showed that failure occurred within the epoxy, close to the primed metal surface as the MFS did not visually appear to be coated with epoxy. This cohesive failure is in agreement with Pike's findings of cohesive failure [1]. Table VI lists the elements detected, the binding energies, and the atomic percents.

In the stress durability test, P/F and CAA surfaces were coated with E-8385. Tables VII and VIII list the elements detected, the binding energies, and the atomic percents. While the primed P/F MFS contained titanium, aluminum and nitrogen were also present. Bromine and nitrogen were present on the AFS as well as aluminum. Similar results were found for the primed CAA failure surfaces. These results suggest two possible mechanisms of failure. Figure 26 shows the two possibilities as the crack hopping from primer to epoxy or as a mixed region of primer and epoxy through which the crack propagates. The locus of failure for the primed P/F and CAA surfaces is not cohesive.

#### SUMMARY

Three alkoxide primers, TNBT, TIPT and E-8385 were studied by XPS, FTIR, STEM and durability testing. Cure temperature affected the alkoxide film thickness and composition. The TNBT and TIPT films were thinner after 300°C cure than 25°C cure. In all films, the C/Al ratio decreased after the 300°C cure. The C-H stretch region disappeared in the 300°C cure films. The effect of solvent moisture content was studied for E-8385 films. The E-8385 films from wet toluene were thinner than the E-8385 films from dry toluene. Silicon contamination present on all brushed films originated from the brush.

Although the topographies of the films looked identical at 6400 X, at 50,000 X extra surface features were seen on the E-8385 films. Bond durability of P/F primed samples differed dramatically. The TNBT and TIPT primed P/F samples showed no enhancement in durability over unprimed P/F samples; however, the E-8385 primed P/F samples showed marked improvement in bond durability over unprimed P/F.

#### REFERENCES

- [1] R. Pike, Int. J. Adhesion and Adhesives 6, 21, 1986.
- [2] B. E. Yoldas, J. Mat. Sci. 21, 1087, 1986.
- [3] B. E. Yoldas, J. Amer. Ceramic Soc. 65, 387, 1982.
- [4] B. E. Yoldas, J. Mat. Sci. 14, 1843, 1979.
- [5] J. A. Filbey and J. P. Wightman, ONR Annual Report, May, 1986.
- [6] J. A. Filbey and J. P. Wightman , ONR Semi-Annual Report, August, 1986.



## APPENDIX A

## Chromic Acid Anodization (CAA)

1. Gritblast with an Econoline gritblaster at approximately 100 psi and held approximately 5 cm from the coupon.
2. Wipe with methyl ethyl ketone (MEK).
3. Soak in sodium hydroxide solution (13 g/250 ml) at 70° C for 5 minutes.
4. Rinse three times in deionized water.
5. Pickling step: Immerse in pickle solution (15 ml conc.  $\text{HNO}_3$ , 3 ml 49% w/w HF, 82 ml  $\text{H}_2\text{O}$ ).
6. Rinse three times in deionized water.
7. Anodize at room temperature for 20 minutes at 10 volts,  $26.9 \text{ amps-m}^{-2}$  ( $2.5 \text{ amps-ft.}^{-2}$ ) in a chromic acid solution (50 g  $\text{CrO}_3$ /1000 ml) with Ti-6-4 as the cathode. 49% w/w HF is added to attain the desired current density.
8. Rinse three times in deionized water, soaking for 5 minutes in the final rinse.
9. Blow dry with prepurified  $\text{N}_2$  gas until visibly dry.

## Phosphate/Fluoride Acidic Etch (P/F)

1. Gritblast as in CAA.
2. Wipe with MEK.
3. Soak in Sprex AN-9 solution (30 g/1000 ml) at 80° C for 15 minutes.
4. Rinse three times in deionized water.
5. Immerse in pickle solution (31 ml 49% w/w HF, 213 ml conc.  $\text{HNO}_3$ /1000 ml) at room temperature for 2 minutes.
6. Rinse three times in deionized water.

7. Soak in phosphate/fluoride solution (50.5 g  $\text{Na}_3\text{PO}_4$ , 20.5 g KF, 29.1 ml 49% w/w HF/1000 ml) at room temperature for 2 minutes.
8. Rinse three times in deionized water.
9. Soak in deionized water at 65°C for 15 minutes.
10. Blow dry as in CAA.

#### TURCO Basic Etch (TURCO)

1. Gritblast as in CAA.
2. Wipe with MEK.
3. Soak in TURCO 5578 solution (37.5 g/1000 ml) at 70-80° C for 10 minutes.
4. Rinse three times in deionized water.
5. Soak in TURCO 5578 solution (380 g/100 ml) at 89-100° C for 10 minutes.
6. Rinse three times in deionized water.
7. Soak in deionized water at 60-70° C for 2 minutes.
8. Blow dry as in CAA.

#### Sodium Hydroxide Anodization (SHA)

1. Gritblast as in CAA.
2. Rinse with methanol or acetone.
3. Immerse in Super Terj (30 g/1000 ml) at 80° C for 15 minutes.
4. Soak in water at 50-60° C for 15 minutes.
5. Anodize at 20° C for 30 minutes at 10 volts in 5.0 M sodium hydroxide solution with Ti-6-4 or stainless steel mesh as the cathode. The current density was not controlled.
6. Rinse in running tap water for 20 minutes.
7. Dry in oven at 60° C for 10 minutes.

Table I  
XPS ANALYSIS OF TNBT ON FERROTYPE PLATES

<u>Cure Temp.</u>	<u>Take-off Angle</u>	<u>Element</u>	<u>B.E.</u>	<u>A.P.</u>	<u>Si/Ti</u>	<u>C/Ti</u>	<u>Cr/Ti</u>	<u>O/Ti</u>
25°C	90°	C	285.	35.				
		O	531.2	46.				
		Ti	459.6	15.	0.24	2.3	0	3.1
		Cr	-	0				
		Si	102.0	3.6				
300°C	90°	C	285.	10.				
		O	530.8	62.				
		Ti	459.4	16.	0.54	0.63	0.18	3.9
		Cr	577.7	2.8				
		Si	102.7	8.6				
	30°	C	285.	13.	0.71	0.93	0.11	4.4
		O	530.9	62.				
		Ti	459.3	14.				
		Cr	577.9	1.5				
		Si	102.7	10.				
	10°	C	285.	28.	1.4	3.5	0.16	6.5
		O	532.4, 530.8	52.				
		Ti	459.2	8.0				
		Cr	577.3	1.3				
		Si	102.6	11.				

Table II  
XPS ANALYSIS OF TIPT ON FERROTYPE PLATES

<u>Cure Temp.</u>	<u>Take-off Angle</u>	<u>Element</u>	<u>B.E.</u>	<u>A.P.</u>	<u>Si/Ti</u>	<u>C/Ti</u>	<u>Cr/Ti</u>	<u>O/Ti</u>
25°C	90°	C	285.	31.	0.44	2.1	0	3.1
		O	531.1	47.				
		Ti	459.5	15.				
		Cr	-	0				
		Si	101.9	6.6				
300°C	90°	C	285.	8.4	0.49	0.49	0.12	3.8
		O	530.9	64.				
		Ti	459.3	17.				
		Cr	577.8	2.0				
		Si	102.6	8.4				
	30°	C	285.0	10.	0.38	0.59	0.05	3.8
		O	530.9	65.				
		Ti	459.4	17.				
		Cr	578.3	0.9				
		Si	102.7	6.4				
	10°	C	285.	20.	0.61	1.7	0.01	5.0
		O	531.4	60.				
		Ti	459.6	12.				
		Cr	577.8	0.6				
		Si	103.0	7.3				

Table III  
XPS ANALYSIS OF E-8385 ON FERROTYPE PLATES

<u>Cure Temp.</u>	<u>Take-off Angle</u>	<u>Element</u>	<u>B.E.</u>	<u>A.P.</u>	<u>Si/Al</u>	<u>C/Al</u>	<u>Cr/Al</u>	<u>O/Al</u>
Dry Toluene	90°	C	285.	21.	0.26	0.88	0.08	2.0
		O	532.5	47.				
		Al	75.0	24.				
		Cr	577.8	1.8				
		Si	102.2	6.3				
	30°	C	285.	23.	0.33	0.96	0.02	1.9
		O	532.5	45.				
		Al	75.4	24.				
		Cr	577.3	0.5				
		Si	102.3	7.9				
	10°	C	285.	36.	0.34	2.6	0	3.2
		O	532.3	45.				
		Al	74.9	14.				
		Cr	-	0				
		Si	101.9	4.8				
	90°	C	285.	20.	0.30	1.0	0.37	2.4
		O	532.2	47.				
		Al	75.8, 74.8	20.				
		Cr	577.3	7.3				
		Si	102.5	6.0				
Wet Toluene	30°	C	285.	25.	0.35	1.3	0.16	2.3
		O	532.7	46.				
		Al	76.2	20.				
		Cr	577.3	3.1				
		Si	102.8	7.0				
	10°	C	285.	31.	0.39	2.1	0.10	3.1
		O	532.7	47.				
		Al	75.4	15.				
		Cr	576.6	1.5				
		Si	102.5	5.8				

Table III, continued

<u>Cure Temp.</u>	<u>Take-off Angle</u>	<u>Element</u>	<u>B.E.</u>	<u>A.P.</u>	<u>Si/Al</u>	<u>C/Al</u>	<u>Cr/Al</u>	<u>O/Al</u>
300°C  Dry Toluene	90°	C	285.	11.	0.14	0.40	0.07	1.8
		O	532.0	53.				
		Al	74.6	29.				
		Cr	577.4	2.1				
		Si	102.4	4.2				
	30°	C	285.	13.	0.16	0.45	0.04	1.8
		O	532.1	52.				
		Al	74.6	29.				
		Cr	577.6	1.2				
		Si	102.4	4.5				
	10°	C	285.	16.	0.11	0.57	0.01	1.9
		O	532.0	53.				
		Al	74.6	28.				
		Cr	578.0	0.4				
		Si	102.4	3.2				
300°C  Wet Toluene	90°	C	285.	7.9	0.35	0.40	0.35	2.9
		O	532.1	57.				
		Al	74.8	20.				
		Cr	577.4	6.9				
		Si	102.9	6.9				
	30°	S	169.8	2.2				
		C	285.	10.	0.43	0.53	0.22	3.1
		O	532.3	58.				
		Al	74.9	19.				
		Cr	577.3	4.1				
		Si	102.8	8.1				
	10°	S	169.3	2.6				
		C	285.	7.8	0.28	0.49	0.16	3.9
		O	532.3	66.				
		Al	74.7	17.				
		Cr	577.5	2.7				
		Si	102.7	4.7				
		S	169.6	2.0				

Table III, continued

Cure Temp.	Take-off Angle	Element	B.E.	A.P.	Si/Al	C/Al	Cr/Al	O/Al
25°C Wet Toluene	90°	C	285.	28.	0	1.6	0.38	2.8
		O	531.9	48.				
		Al	74.4	17.				
		Cr	577.2	6.5				
		Si	-	trace				
Spun Coat	30°	C	285.	35.	0.07	2.1	0.16	2.5
		O	532.1	43.				
		Al	74.3	17.				
		Cr	577.4	2.7				
		Si	101.9	1.1				
	10°	C	285.	39.	0.07	2.3	0.10	2.4
		O	532.0	41.				
		Al	74.2	17.				
		Cr	577.6	1.7				
		Si	102.0	1.1				
<hr/>								
300°C Wet Toluene	90°	C	285.	12.	0.07	2.0	0.36	2.2
		O	531.3	53.				
		Al	74.8	24.				
		Cr	577.3	8.7				
		Si	102.2	1.6				
Spun Coat	30°	C	285.	15.	0.08	0.63	0.26	2.2
		O	531.9	53.				
		Al	74.7	24.				
		Cr	577.3	6.2				
		Si	102.7	1.8				
	10°	C	285.	23.	0.10	1.4	0.28	3.2
		O	532.1	54.				
		Al	74.7	17.				
		Cr	577.4	4.8				
		Si	102.4	1.7				

Table IV

XPS ANALYSIS FOR LOCUS OF FAILURE OF P/F BONDS EXPOSED TO  
80°C 95% RH

<u>Surface</u>	<u>Element</u>	<u>B.E.</u>	<u>A.P.</u>
MFS Wedge Test	C	285.	43.
	O	529.4	36.
	Ti	458.1	9.1
	N	399.6	9.8
	Ca	347.	1.5
	Br	-	none
	P	-	none
AFS Wedge Test	C	285.	91.
	O	532.4	8.2
	Br	71.7	0.5
	N	-	trace
	Ti	-	none
MFS Stress Durability Test	C	285.	73.
	O	529.8	21.
	Ti	458.5	4.3
	Ca	348.5	1.7
	Br	-	none
	P	-	trace
AFS Stress Durability Test	C	285.	85.
	O	532.1	13.
	Br	71.6	0.7
	N	399.6	1.4
	Ti	-	none



Table V

XPS ANALYSIS FOR LOCUS OF FAILURE OF TURCO  
BONDS EXPOSED TO 80°C 95% RH

<u>Surface</u>	<u>Element</u>	<u>B.E.</u>	<u>A.P.</u>
AFS Stress Durability Test	C	285.	78.
	O	532.7	17.
	Br	70.9	0.6
	N	400.1	2.2
	Al	120.2	2.7
	Ti	---	none
MFS Stress Durability Test	C	285.	62.
	O	531.9, 529.8	33.
	Ti	458.4	2.4
	Ca	347.7	1.5
	Na	1071.8	0.5
	Fe	---	trace

Table VI

XPS ANALYSIS FOR LOCUS OF FAILURE OF P/F WITH TNBT FROM  
 DRY TOLUENE 25°C CURE EXPOSED TO 80°C, 95% RH

<u>Surface</u>	<u>Element</u>	<u>B.E.</u>	<u>A.P.</u>
MFS Wedge Test	C	285.	92.
	O	533.0	5.9
	Ti	-	none
	Br	70.9	0.3
	Si	102.2	1.3
	N	-	trace
AFS Wedge Test	C	285.	89.
	O	533.1	8.8
	Br	71.0	0.8
	N	400.1	0.9
	Si	102.3	0.5

Table VII

XPS ANALYSIS FOR LOCUS OF FAILURE OF P/F WITH E-8385 FROM  
 DRY TOLUENE, 25° CURE EXPOSED TO 80°C 95% RH

<u>Surface</u>	<u>Element</u>	<u>B.E.</u>	<u>A.P.</u>
MFS	C	285.	46.
Stress	O	530.6, 533.0	37.
Durability	Br	-	trace
Test	N	400.3	5.8
	Al	74.7	5.6
	Ti	459.0	4.7
AFS	C	285.	75.
Stress	O	532.7	20.
Durability	Br	70.7	0.4
Test	N	399.7	1.7
	Al	75.0	3.4
	Ti	-	none

Table VIII

XPS ANALYSIS FOR LOCUS OF FAILURE OF CAA WITH E-8385 FROM  
 DRY TOLUENE, 25°C CURE EXPOSED TO 80°C, 95% RH

<u>Surface</u>	<u>Element</u>	<u>B.E.</u>	<u>A.P.</u>	<u>O/Al</u>
MFS 1 Stress Durability Test	C	285.	34.	2.5
	O	532.1	42.	
	Ti	458.3	1.0	
	Br	-	trace	
	Al	74.5	17.	
	N	399.8	5.2	
	F	685.8	0.6	
MFS 2 Stress Durability Test	C	285.	56.	6.7
	O	531.0, 530.0	33.	
	Ti	457.6	5.4	
	Br	-	trace	
	Al	73.4	4.9	
	N	-	trace	
	F	-	none	
AFS 1 Stress Durability Test	C	285.	62.	2.9
	O	532.7	25.	
	Ti	-	trace	
	Br	70.8	1.1	
	Al	74.7	8.6	
	N	400.1	2.9	
	F	685.8	0.6	
AFS 2 Stress Durability Test	C	285.	30.	2.0
	O	531.8	45.	
	Ti	-	trace	
	Br	-	trace	
	Al	74.1	23.	
	N	399.3	1.6	
	F	685.3	0.6	

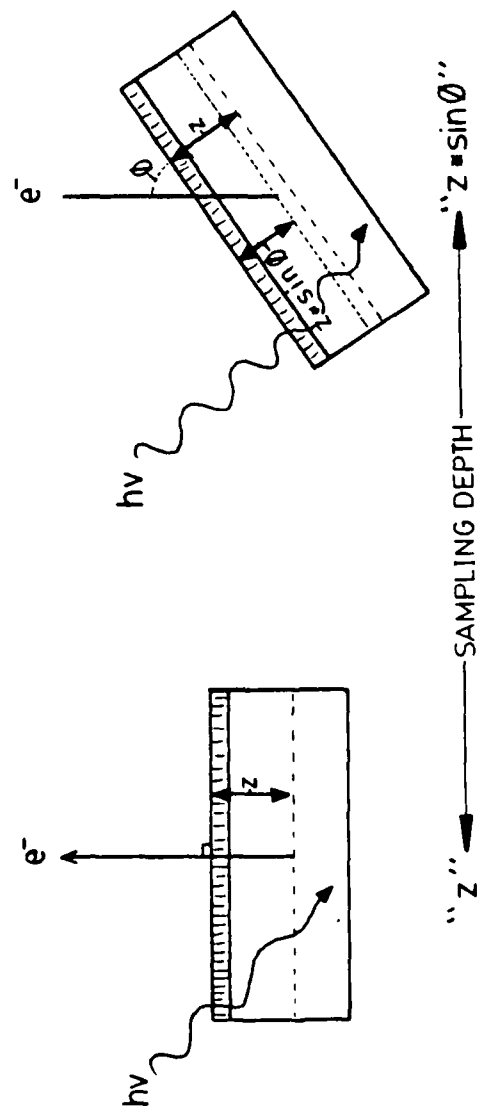


Figure 1. Schematic diagram of XPS angular analysis

## Grazing Angle Reflectance Accessory

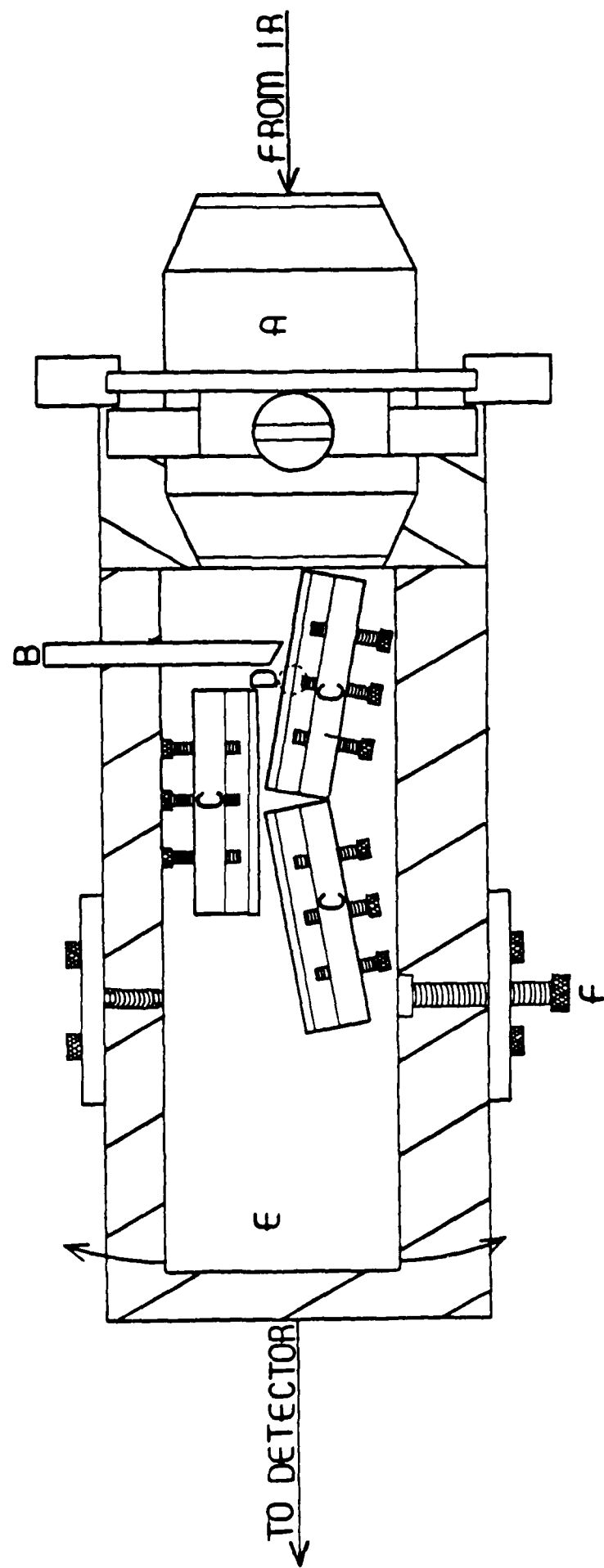


Figure 2. Grazing angle specular reflectance attachment for the Nicolet 5DX FTIR

## STRESS DURABILITY TEST

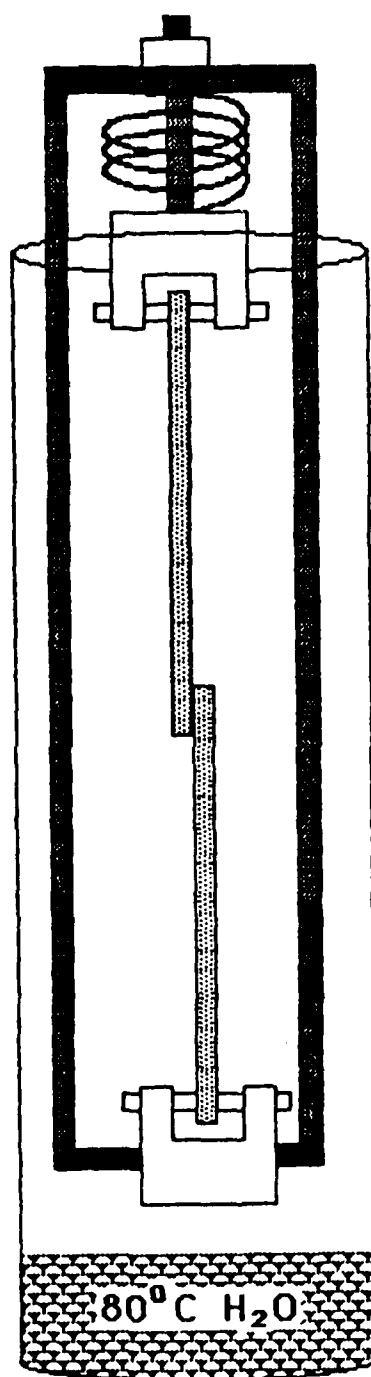


Figure 3. Schematic diagram of stress-durability test cell

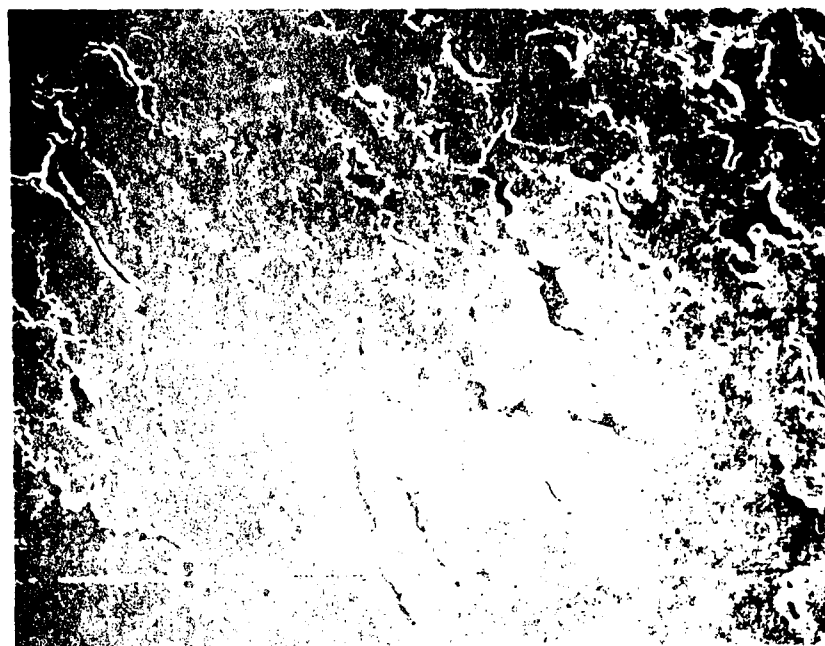


Figure 4. STEM photomicrograph at 6400 X of TNBT on Ti-6-4, cured at 25°C

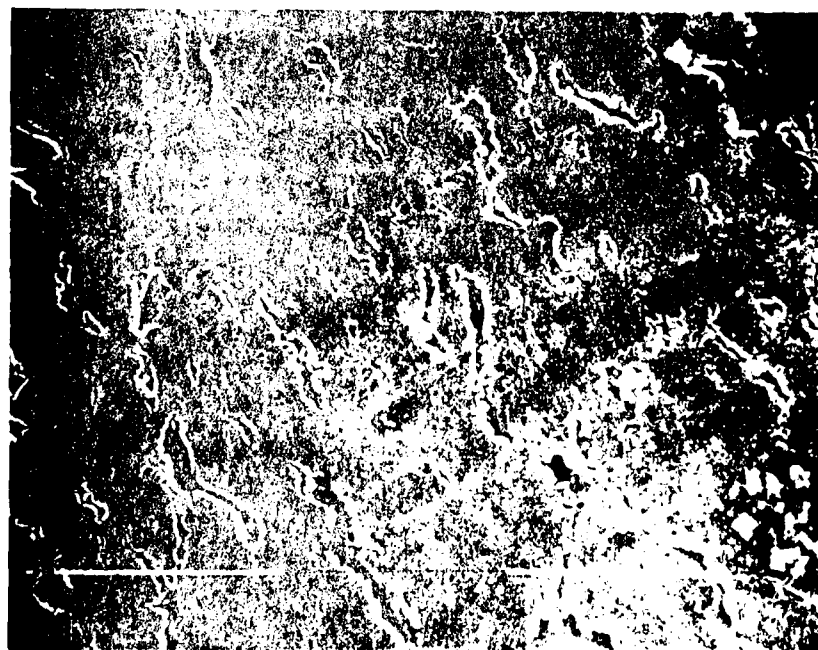


Figure 5. STEM photomicrograph of 6400 X of E-8385 from dry toluene on Ti-6-4 cured, at 25°C



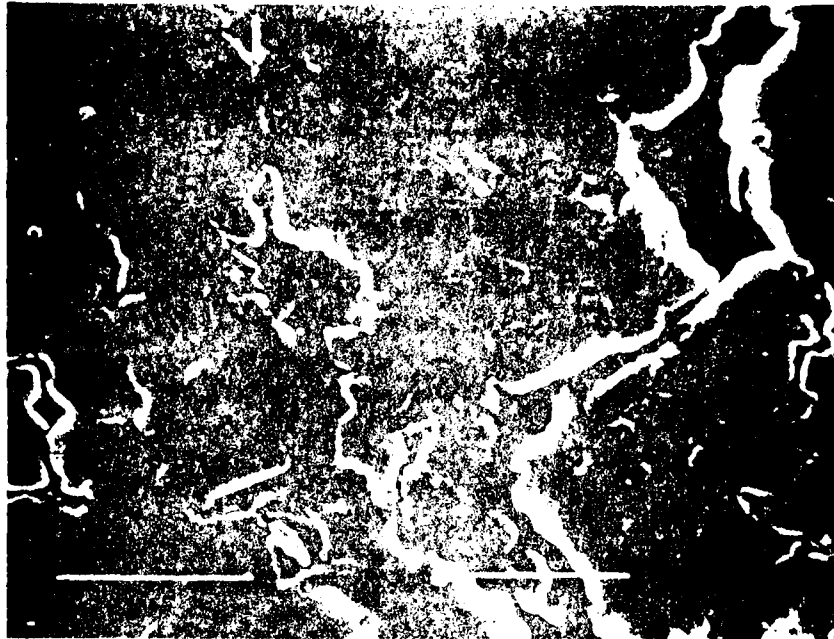


Figure 6. STEM photomicrograph of 50,000 X of TNBT on Ti-6-4, coated at 25°C.

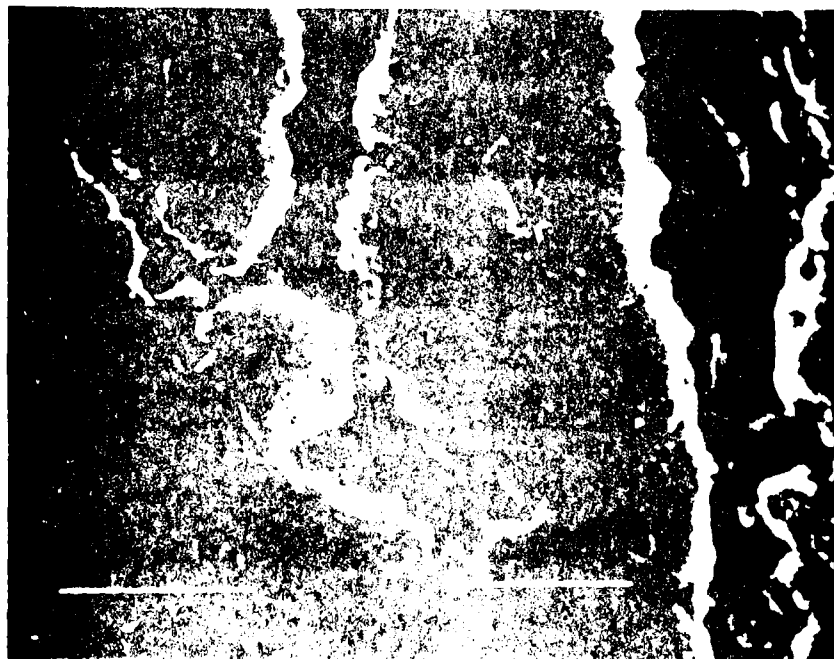


Figure 7. STEM photomicrograph of 50,000 X of TNBT on Ti-6-4, coated from dry solvent at 25°C.

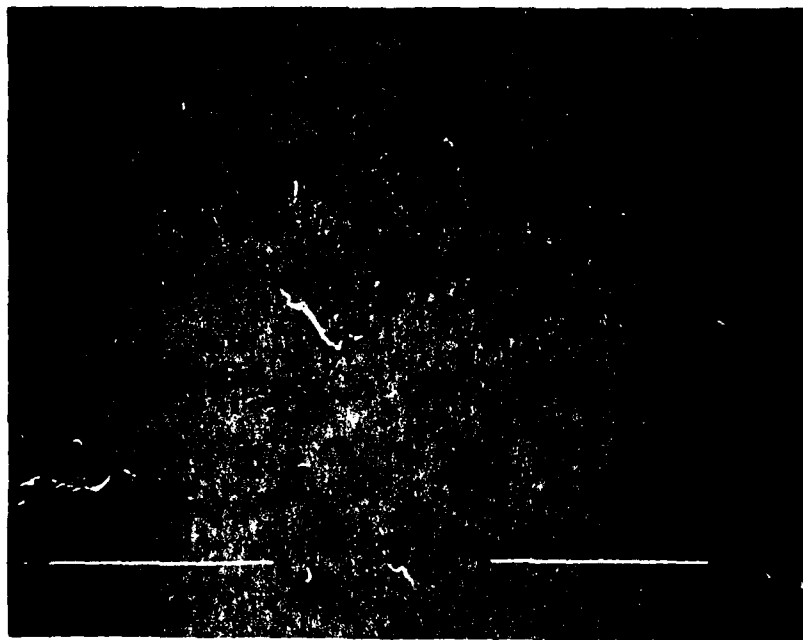


Figure 8. STEM photomicrograph at 6400 X of TNBT on Ti-6-4, cured at 300°C.

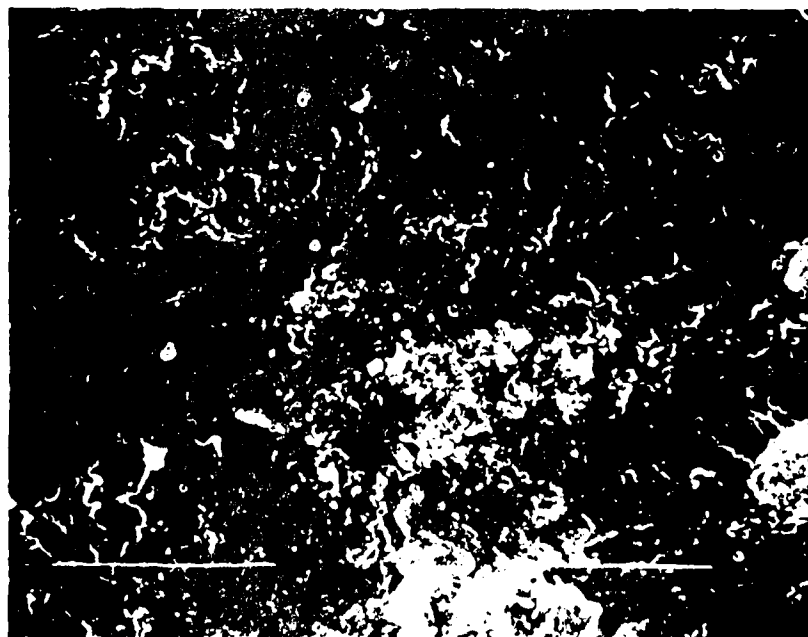


Figure 9. STEM photomicrograph at 6400 X of E-8385 from dry toluene on Ti-6-4, cured at 300°C.



Figure 10. STEM photomicrograph at 50,000 X of TNBT on Ti-6-4, cured at 300°C.

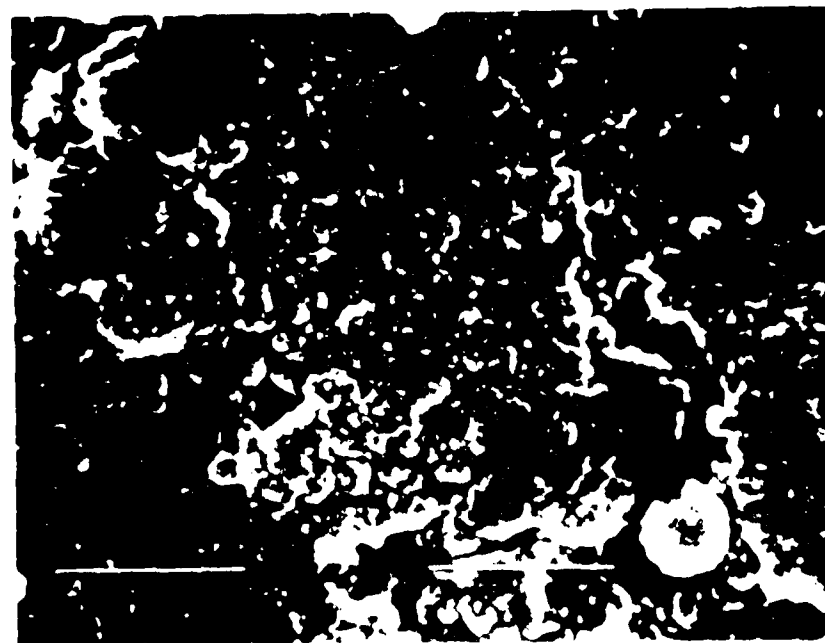


Figure 11. STEM photomicrograph at 50,000 X of c-8385 from dry toluene on Ti-6-4, cured at 300°C.

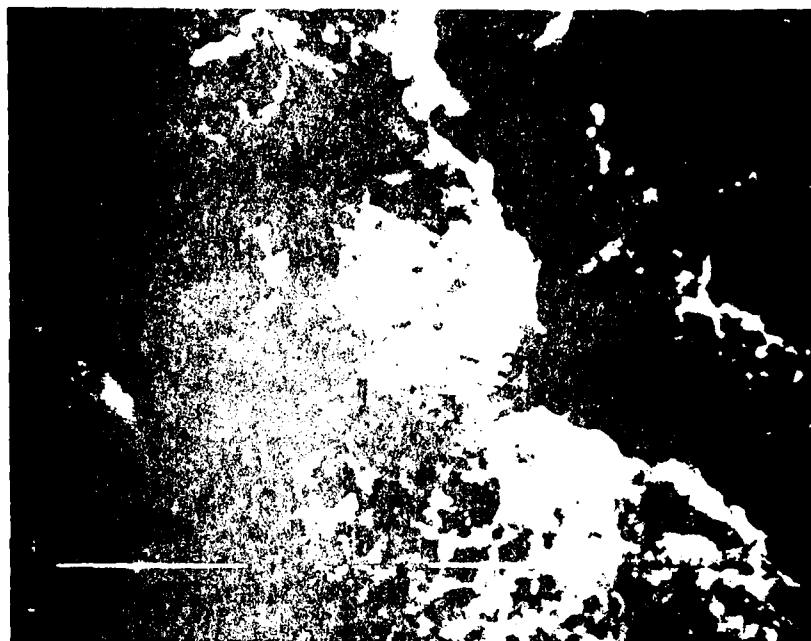


Figure 12. STEM photomicrograph at 50,000 X of E-8385 from wet toluene on Ti-6-4, cured at 25°C.

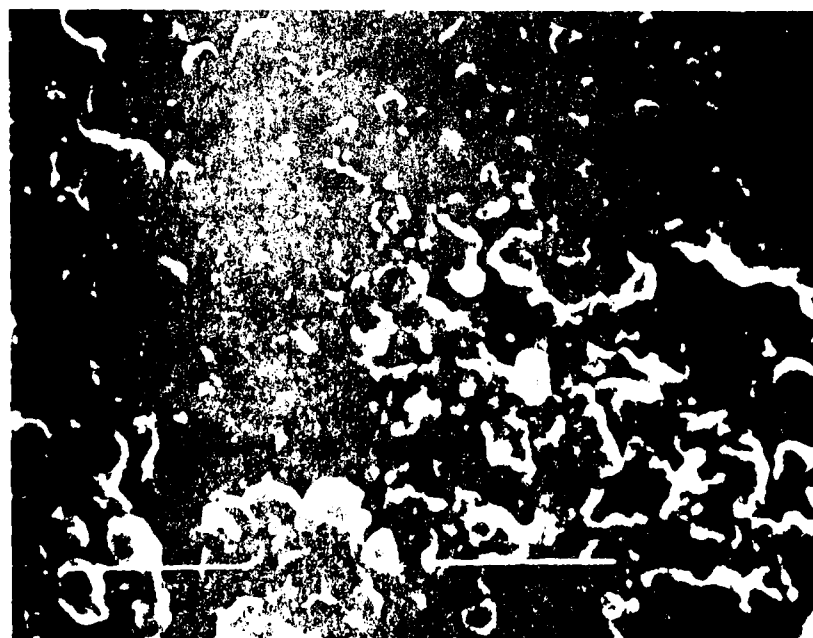


Figure 13. STEM photomicrograph at 50,000 X of E-8385 from wet toluene on Ti-6-4, cured at 300°C.

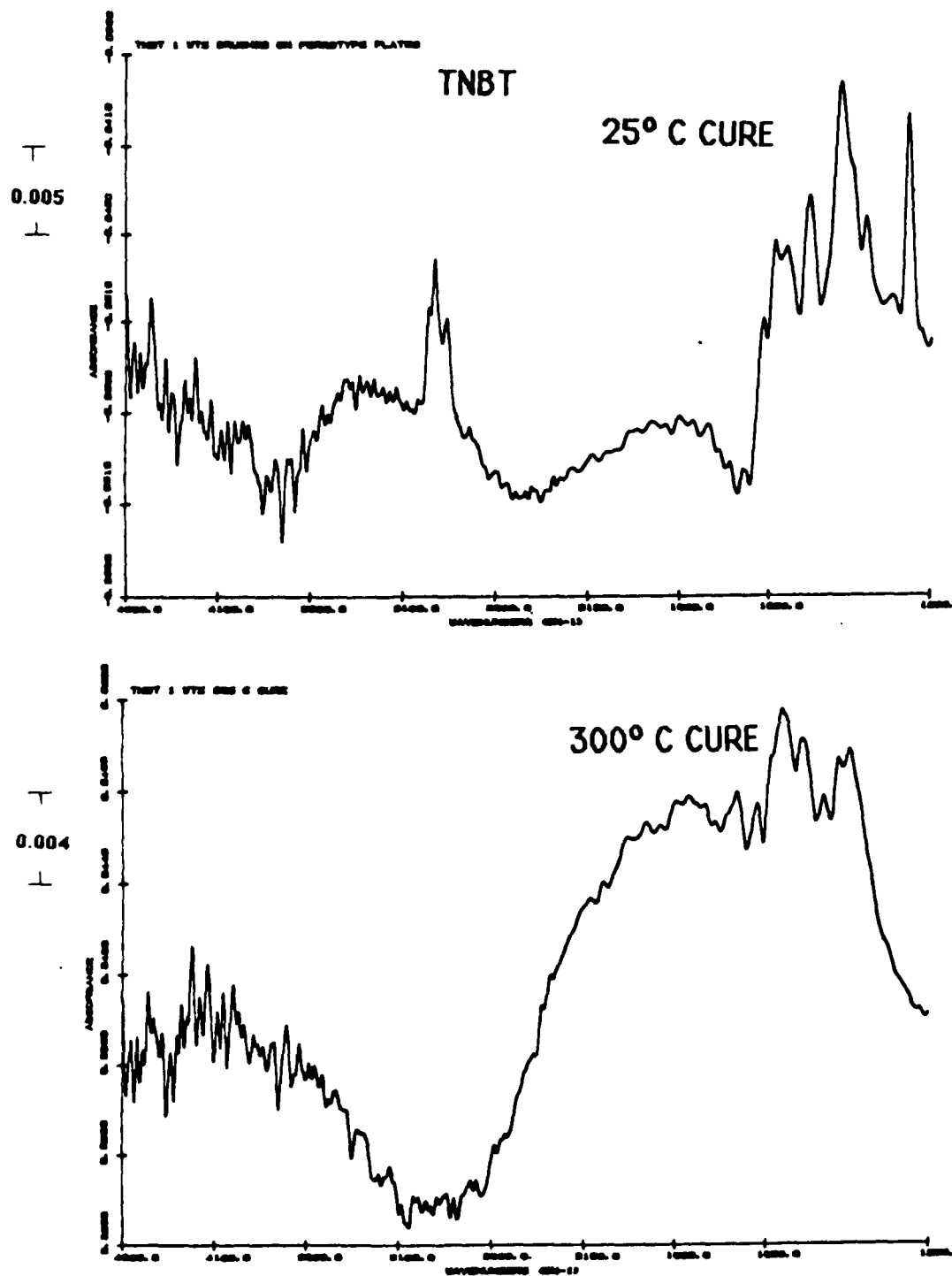


Figure 14. Grazing angle FTIR spectra from 4600 to 1200  $\text{cm}^{-1}$  of TNBT on ferrotypes plates, cured at 25° and 300°C

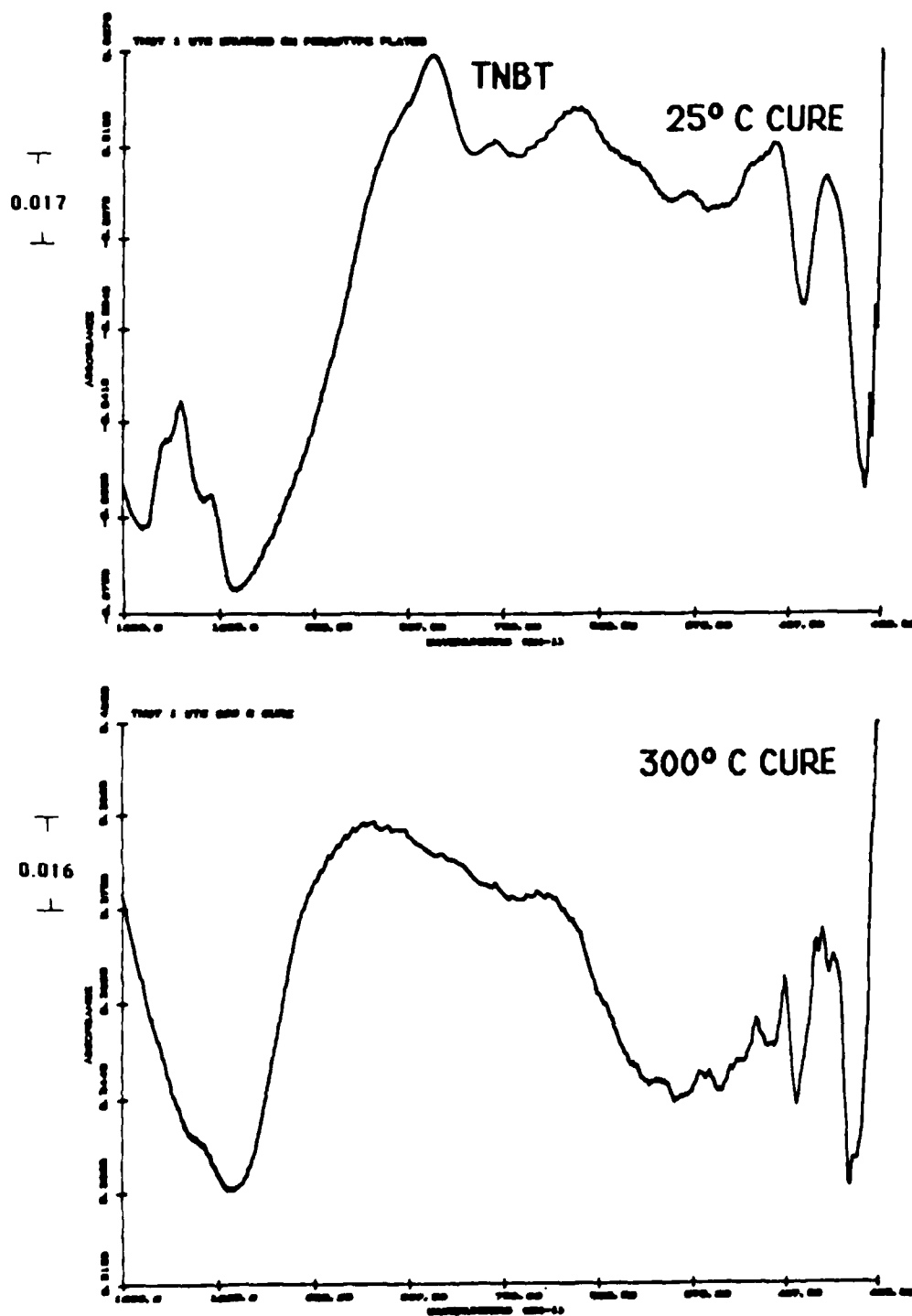


Figure 15. Grazing angle FTIR spectra from 1200 to 400  $\text{cm}^{-1}$  of TNBT on ferrotypes plates, cured at 25° and 300°C

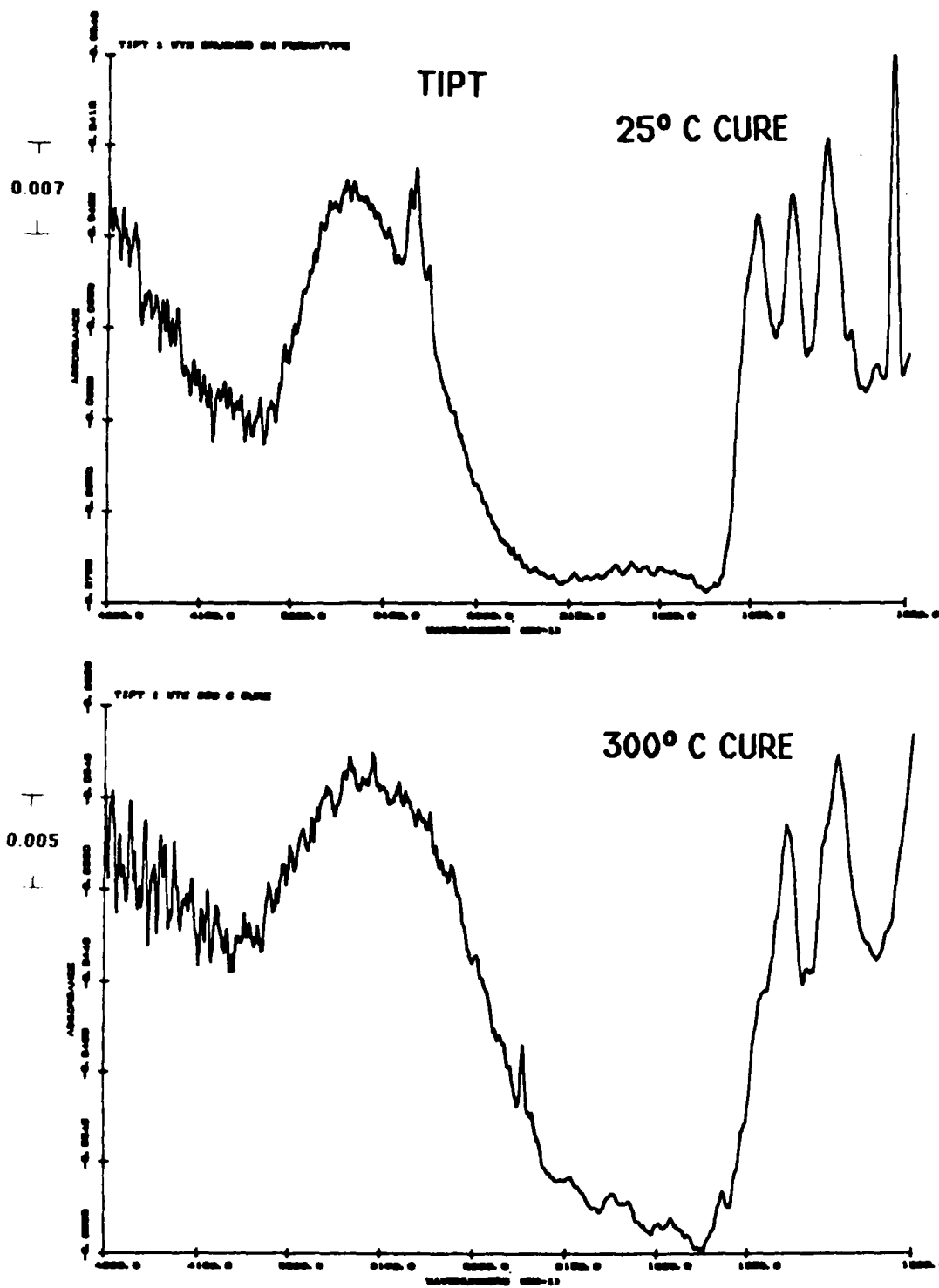


Figure 16. Grazing angle FTIR spectra from 4600 to 1200  $\text{cm}^{-1}$  of TIPT on ferrotypes plates, cured at 25° and 300°C

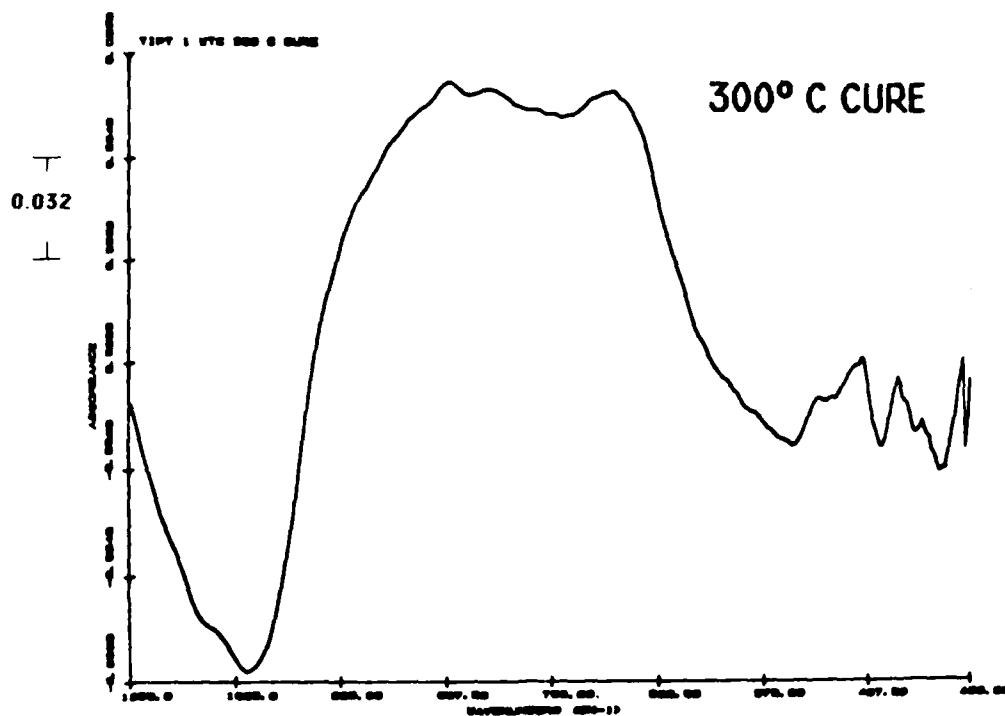
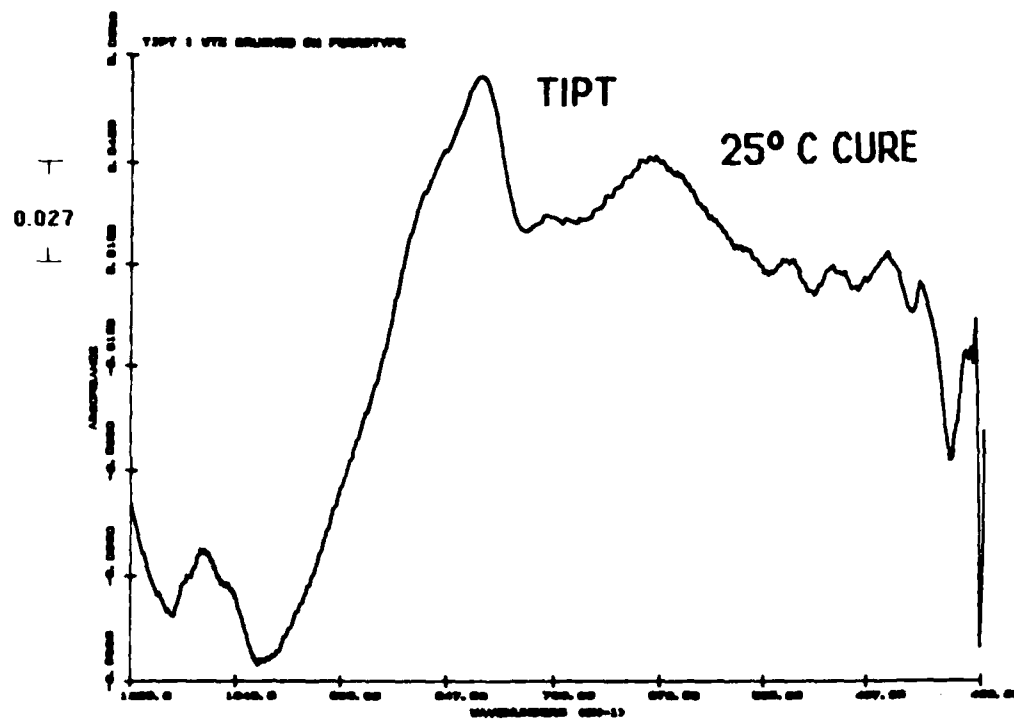


Figure 17. Grazing angle FTIR spectra from 1200 to 400  $\text{cm}^{-1}$  of TIPT on ferrotyp plates, cured at 25° and 300°C



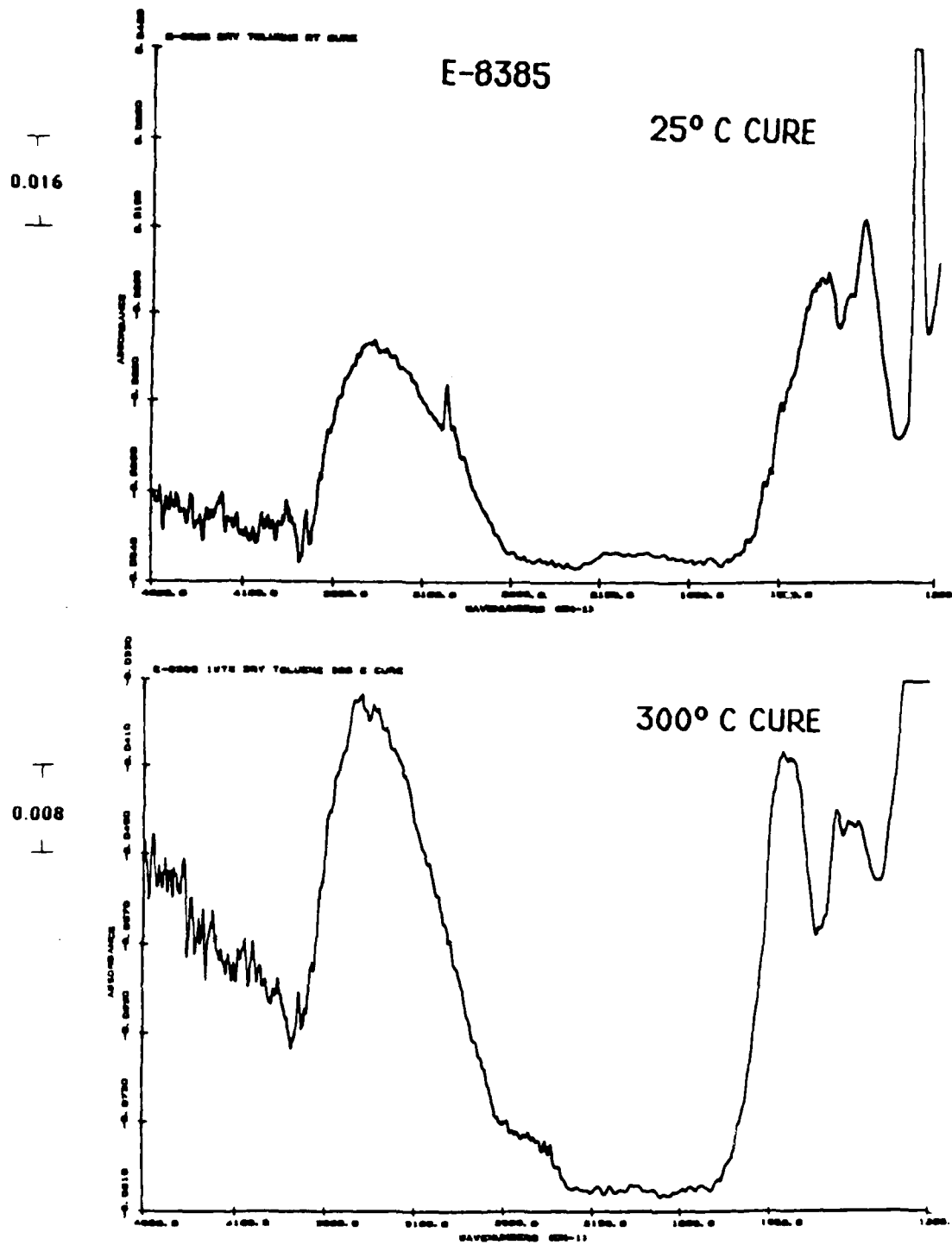


Figure 18. Grazing angle FTIR spectra from 4600 to 1200  $\text{cm}^{-1}$  of E-8385 from dry toluene on ferrotype plates, cured at 25°C and 300°C

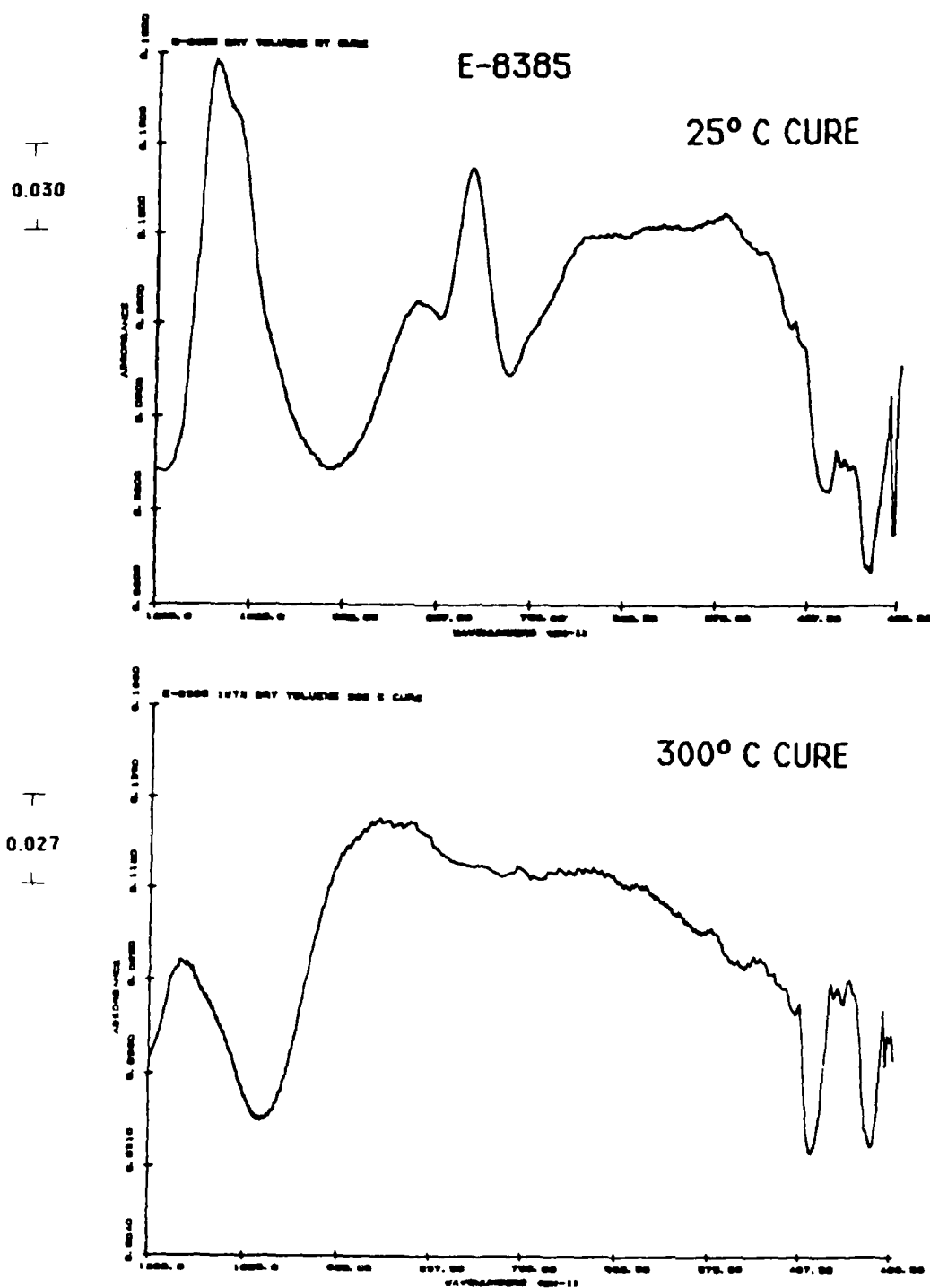


Figure 19. Grazing angle FTIR spectra from 1200 to 400  $\text{cm}^{-1}$  of E-8385 from dry toluene on ferrotypes plates, cured at 25° and 300°C

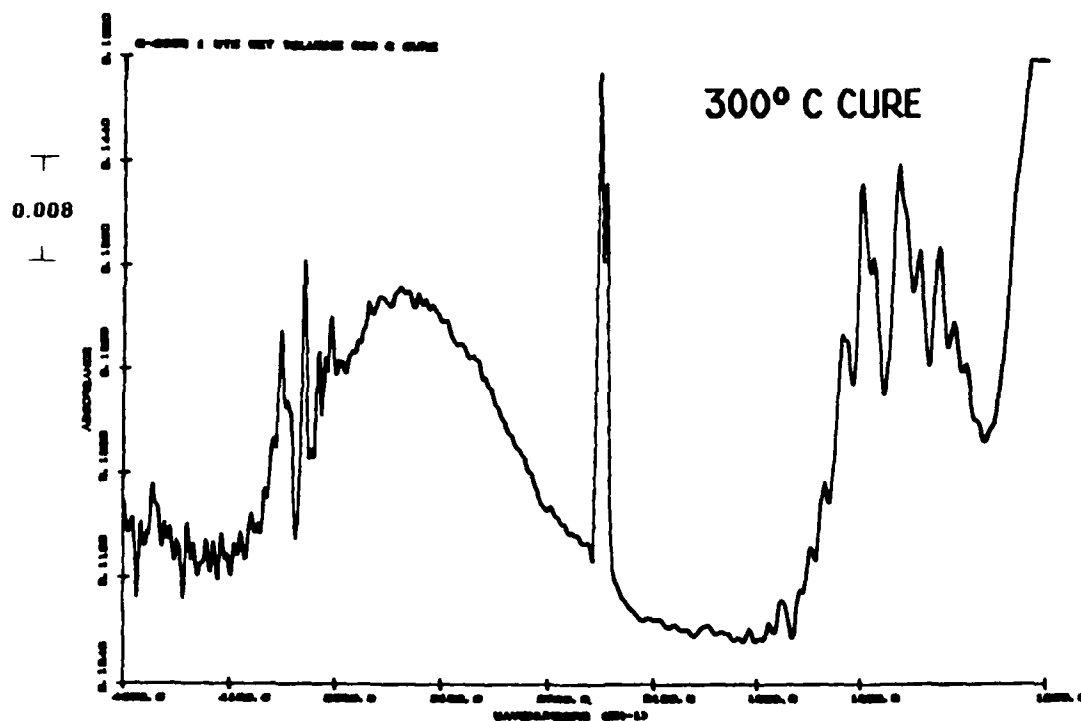
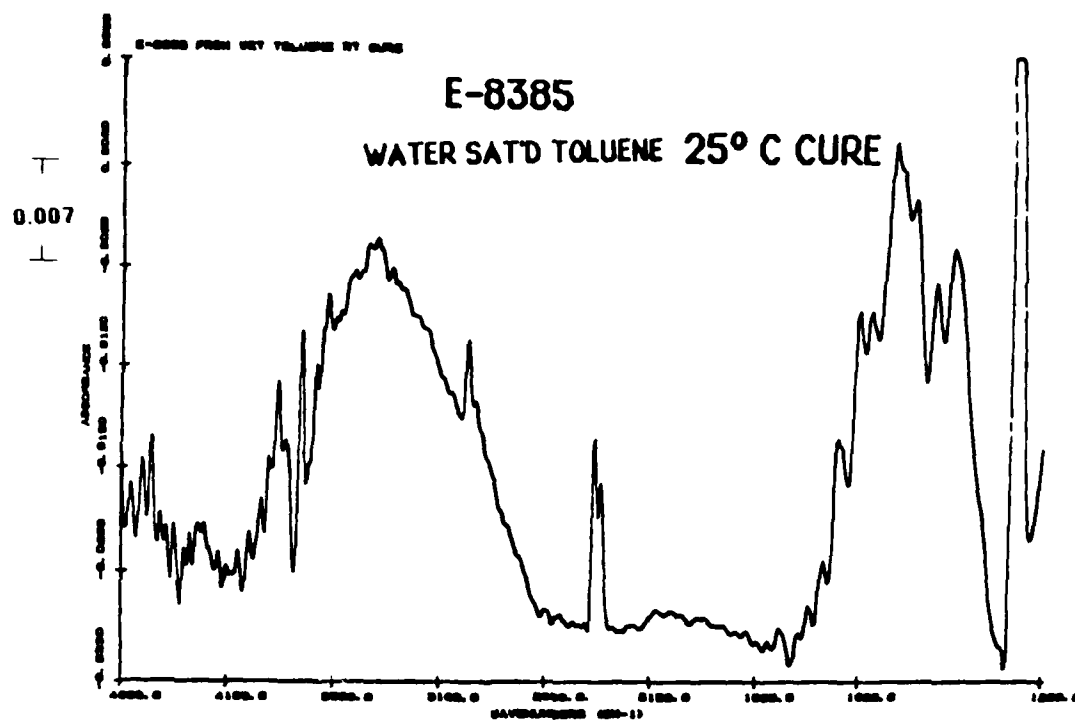


Figure 20. Grazing angle FTIR spectra from 4600 to 1200  $\text{cm}^{-1}$  of E-8385 from wet toluene on ferrotypes plates, cured at 25° and 300°C

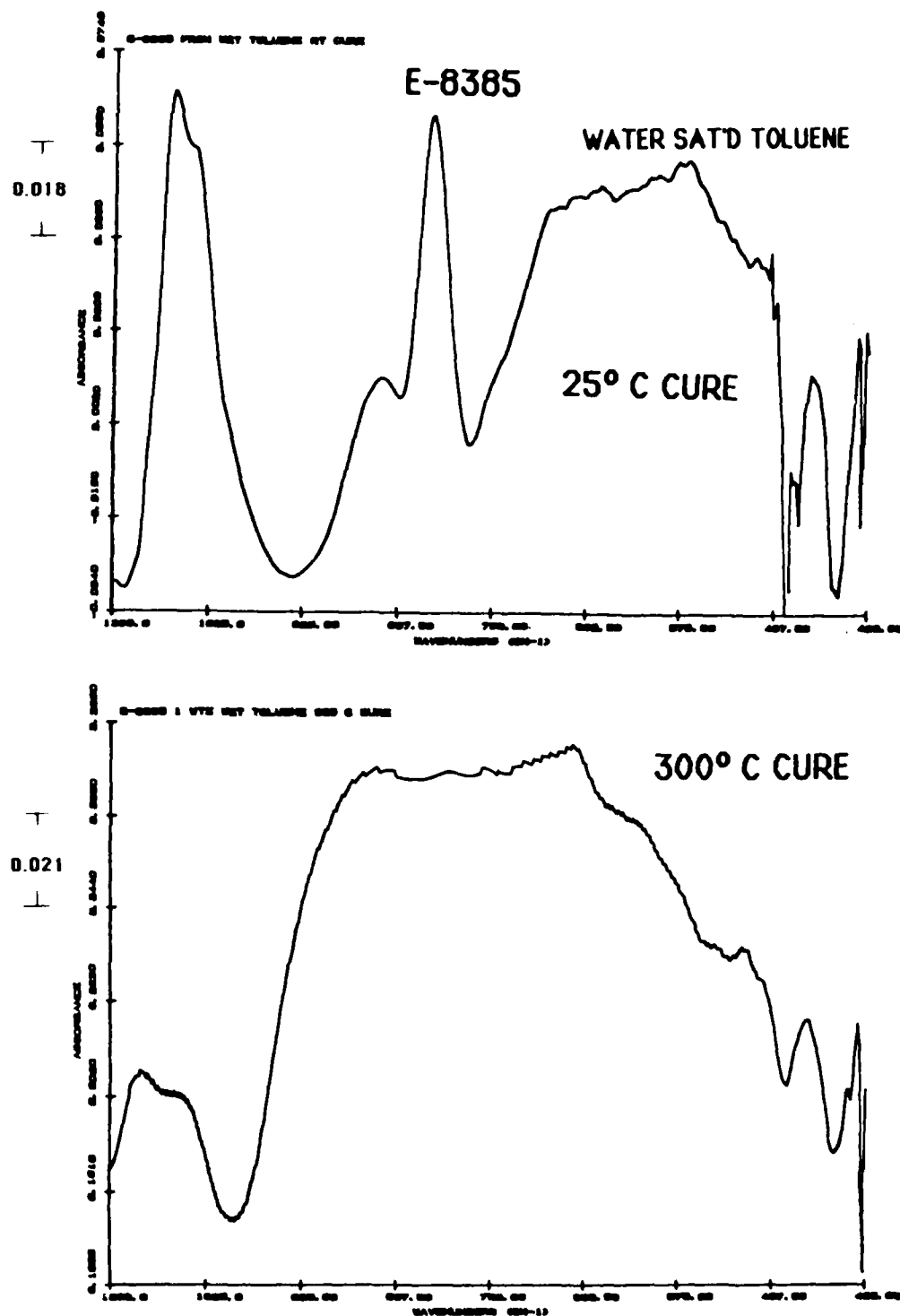


Figure 21. Grazing angle FTIR spectra from 1200 to 400  $\text{cm}^{-1}$  of E-8385 from wet toluene on ferrotype plates, cured at 25° and 300°C

# Wedge Test Titanates

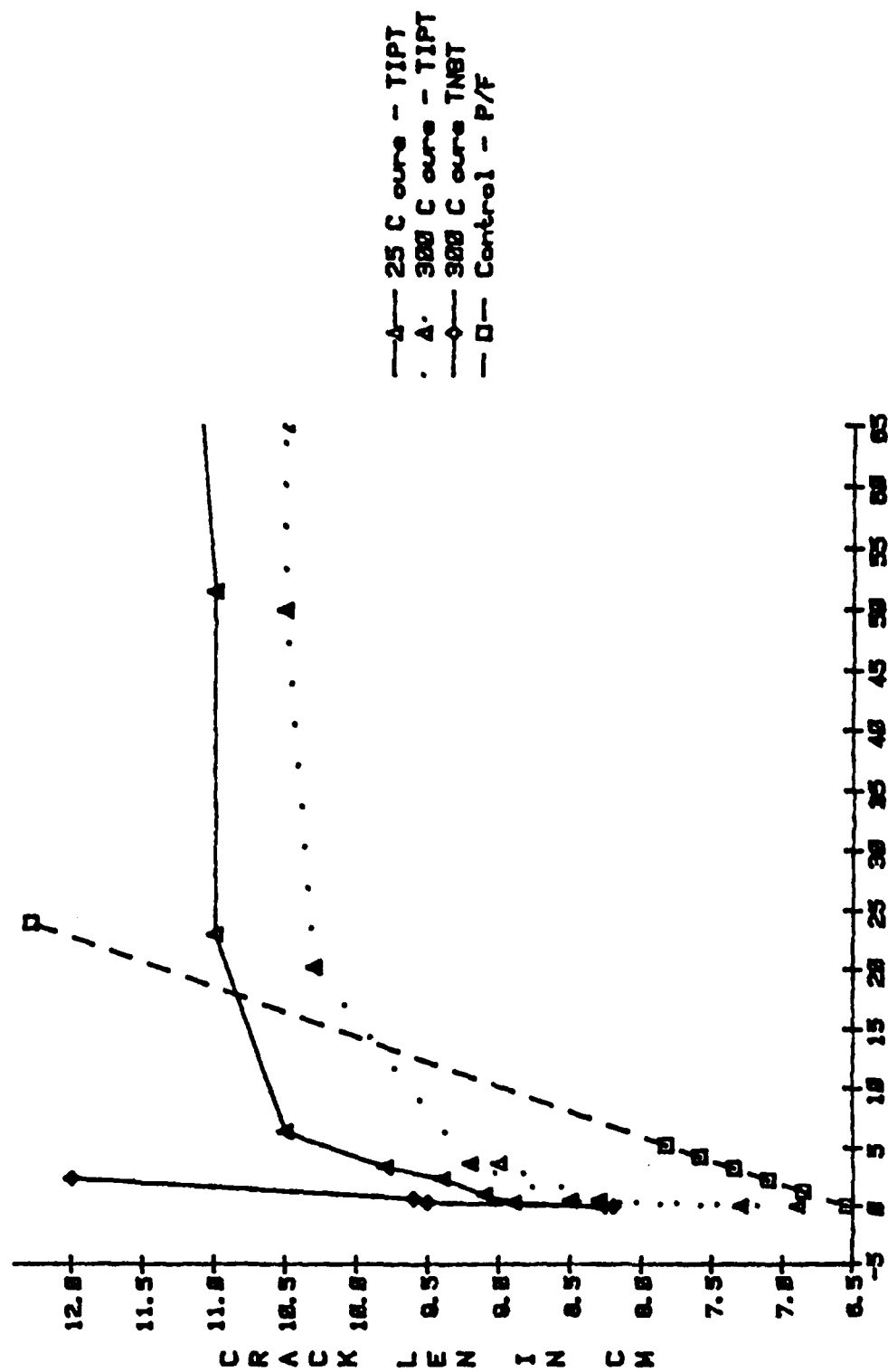


Figure 22. Crack length vs. time for wedge test of TNBT and TIPT primed P/F samples exposed to 80°C 95% r.h.

# E-8385 ON P/F IN 80° C 95% R.H.

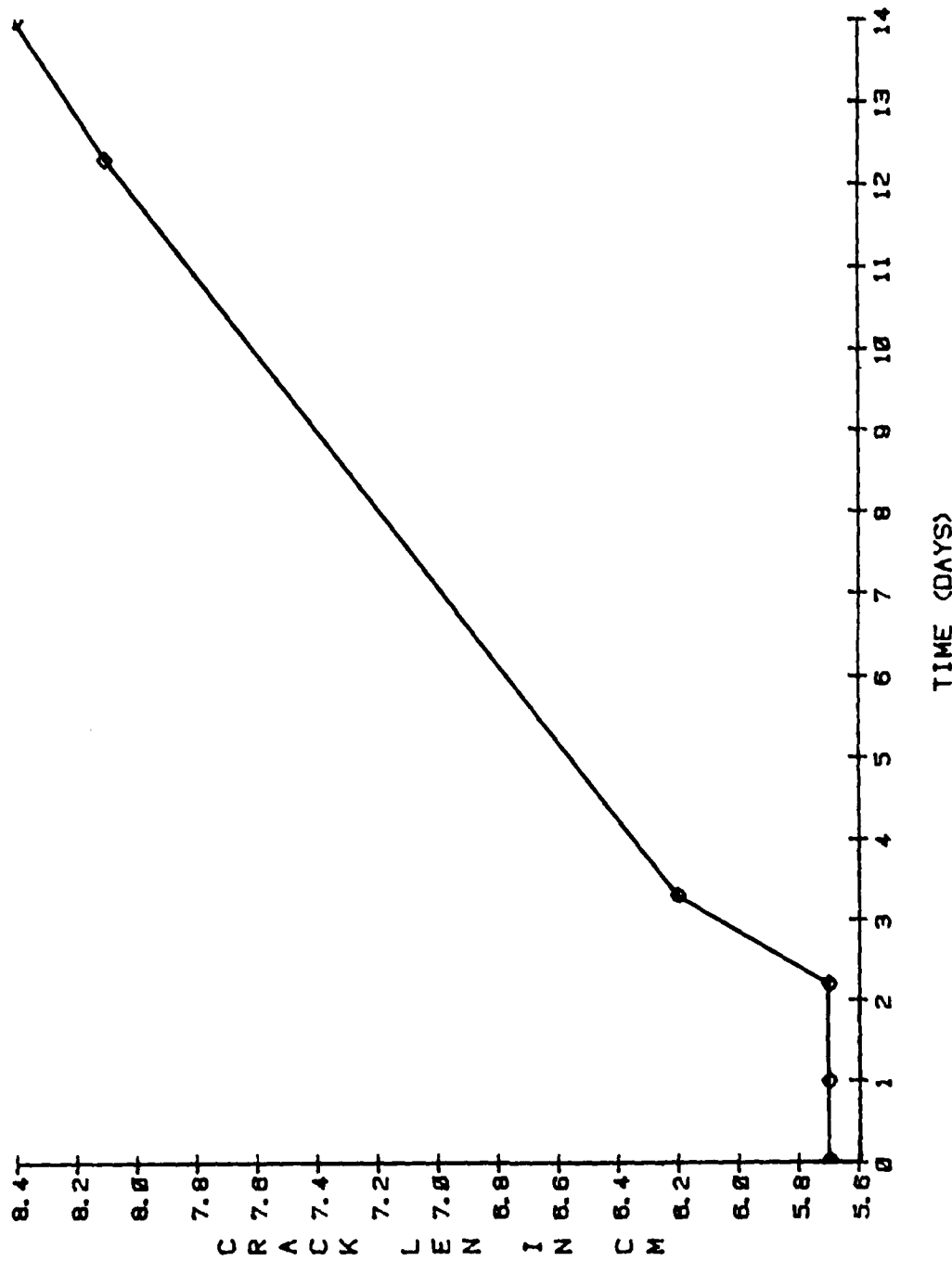


Figure 23. Crack length vs. time for wedge test of E-8385 primed P/F samples exposed to 80°C 95% r.h.

# STRESS DURABILITY TEST

## TIME TO FAILURE

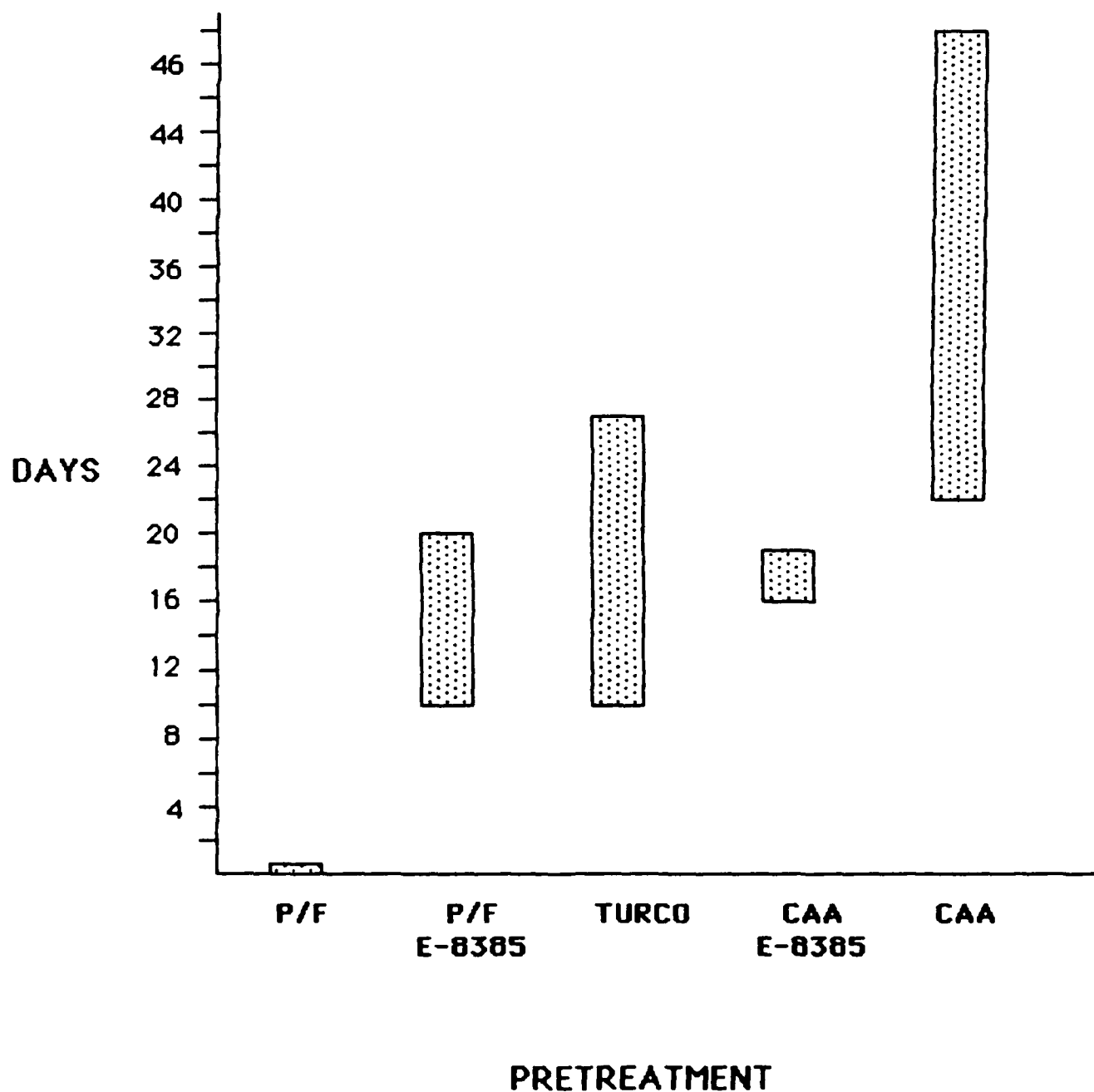


Figure 24. Time to failure windows from stress-durability test at 80°C 95% r.h.

# LOCUS OF FAILURE

P/F

## STRESS DURABILITY AND WEDGE TESTS

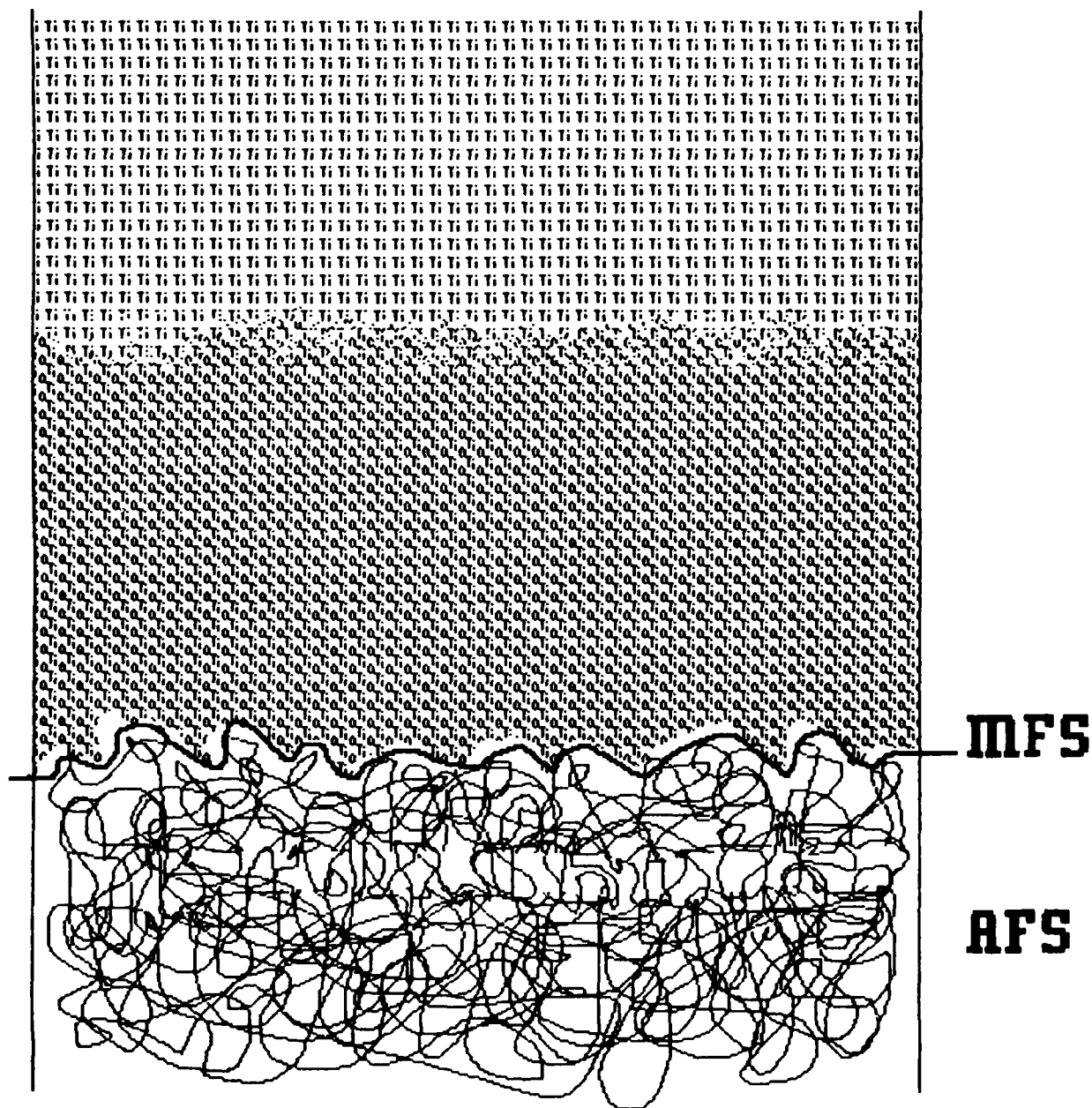


Figure 25. Schematic diagram of locus of failure for P/F pre-treated wedge and stress-durability test samples.



LOCUS OF FAILURE  
P/F & CAA WITH E-8385  
STRESS DURABILITY TEST

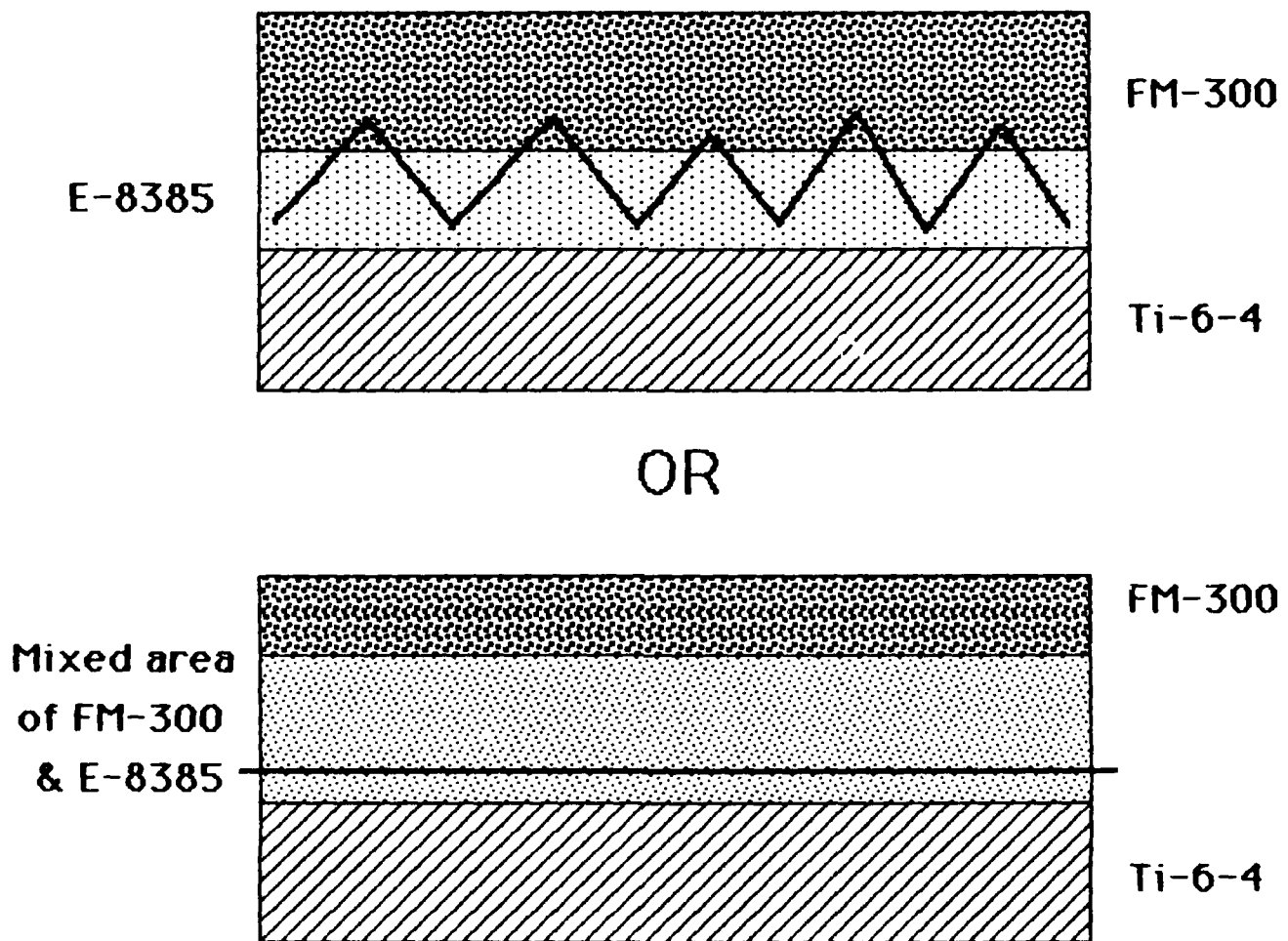


Figure 26. Schematic diagram of two possible mechanisms in the locus of failure for E-8385 primed CAA and P/F pretreated stress durability test samples.

<b>BIBLIOGRAPHIC DATA SHEET</b>	1. Report No.	CAS/CHEM-12	2.	3. Recipient's Accession No.
	CAS/CHEM-86-13 -86, No. 95			
4. Title and Subtitle An Interdisciplinary Approach to Predictive Modeling of Structural Adhesive Bonding Characterization of Ti-6Al-4V Oxides and the Adhesive/Oxide Interphase				5. Report Date
				6.
7. Author(s)				8. Performing Organization Rept. No. CAS/CHEM-96-13 CAS/CHEM-12
9. Performing Organization Name and Address Virginia Polytechnic Institute & State University Center for Adhesion Science and Department of Engineering Science and Mechanics Blacksburg, VA 24061				10. Project/Task/Work Unit No. -86, No. 95
				11. Contract/Grant No. N00014-82-K-0185 P00002
12. Sponsoring Organization Name and Address Office of Naval Research 800 N. Quincy Street Arlington, VA 22217				13. Type of Report & Period Covered Annual Report 3/86-9/86
				14.
15. Supplementary Notes Annual Report				
16. Abstracts				
17. Key Words and Document Analysis, 17a. Descriptors				
17b. Identifiers/Open-Ended Terms				
17c. COSATI Field Group				
18. Availability Statement Unlimited			19. Security Class (This Report) UNCLASSIFIED	21. No. of Pages 44
			20. Security Class (This Page) UNCLASSIFIED	22. Price

END

2-87-

DTIC